Analytical Modeling of Emulsion Flow at the Edge of Steam Chamber During SAGD Process

by

Mahdie Mojarad

A thesis submitted in partial fulfillment of the requirements for the degree of

Master of Science

in
Petroleum Engineering

Department of Civil and environmental Engineering
University of Alberta

Abstract

Different models have been proposed to describe two- and three-phase flow at the edge of a steam chamber developed during a SAGD process. However, two-dimensional scaled SAGD experiments and recent micro model visualizations demonstrate that steam-condensate is primarily in the form of microbubbles dispersed in the oil phase (water-in-oil emulsion). Therefore, the challenging question is: Can multiphase Darcy equation be used to describe the transport of water as a discontinuous phase? Furthermore, the physical impact of water as a continuous phase or as microbubbles on oil flow can be different. Water microbubbles increase the apparent oil viscosity, while a continuous water phase decreases the oil relative permeability. Investigating the impact of these two phenomena on oil mobility at the steam chamber edge and on overall oil production rate during a SAGD process requires development of relevant mathematical models that is the focus of this thesis.

In this thesis, we develop an analytical model for lateral expansion of steam chamber that accounts for formation and transport of water-in-oil emulsion both in single and two phase flow. It is assumed that emulsion is generated due to condensation of steam, which is penetrated into the heated bitumen. The emulsion concentration decreases from a maximum value at the chamber interface to zero far from the interface. The oil viscosity is affected by both temperature gradient due to heat conduction and microbubble concentration gradient due to emulsification. We conduct a sensitivity analysis by using the measured data from scaled SAGD experiments. The sensitivity analysis shows that by increasing the value of m (temperature viscosity parameter), the effect of emulsification on oil flow rate decreases. It also shows that the effect of temperature on oil mobility is much stronger than that of emulsion. We also compare the model predictions with field

production data from several SAGD operations. Butler's model overestimates oil production rate due to single-phase assumption, while the proposed model presents more accurate oil flow rate supporting the fact that emulsification effect should be included in the SAGD analysis.

Dedication

Dedicated to my beloved family,

for their endless love and support.

Acknowledgment

I would like to express my sincere gratitude to my supervisor, Dr. Hassan Dehghanpour, for his trust and confidence in me and for the direction and encouragement throughout the course of this work. His invaluable guidance and personal characteristics have inspired me to question and learn. He has provided me so much more assistance than deserved.

I would also like to thank all the members of our group particularly Ali, Ashkan, Mahmood and Obina for their support.

My love and special thanks go to my family.

Table of Content

List of Tables

List of Figures

1 Chapter One: Introduction

In this chapter, an overview of Canada's heavy oil distribution and related recovery methods are described. Motivations, objectives and outline of the thesis are discussed in the chapter as well.

1.1 Heavy Oil and Oil Sands

Unconventional sources of oil such as heavy oil and oil sands (tar sands) are important hydrocarbon resources that play an increasingly important role in the oil supply of the world. Figure 1 shows the distribution of the world oil resources. The amount of total unconventional oil is about three times the amount of conventional oil in place, which is about 3 trillion barrels worldwide discovered today. Conventional oil is defined as oil with an API gravity of 25° or higher, while unconventional oil, which includes heavy oil and oil sands crude, is characterized by high viscosity and density at reservoir conditions: heavy oil (μ~100−10000 cp, ρ~20°−10°API gravity) and oil sands (μ > 10000 cp, ρ < 10°API gravity). Most heavy oil occurs in shallow (1000 m or less), high permeability (1 to 7 Darcy), high porosity (around 30%), poorly consolidated sand formations (Farouq Ali, 2008). The oil saturations are typically high (50−80%) and formation thicknesses are 10 to several meters (Farouq Ali 2008).

Canada does not have much conventional crude but it does have huge quantities of oil sands, and heavy oil. More than half of Canada oil production is from oil sands. Alberta oil sands contain about two trillion barrels of recoverable heavy oil and bitumen, most of it with in-situ viscosities in the hundreds of thousands to millions of centipoise (cp) at reservoir conditions. The efficient and economic recovery method is a major challenge (Sharma and Gates 2010).

1.2 In-situ Extraction of Heavy Oil

Conventional recovery methods are rarely applicable in high viscosity and low solution gas content which are the characteristics of heavy oil and oil sands. Primary recovery factors are low, averaging about 5% of the oil-in-place (Farouq Ali, 2008). Recovery processes include thermal and non-thermal methods.

1.2.1 Non-thermal Recovery Methods

Non-thermal heavy oil recovery techniques can be considered for moderate viscous oils (50-200 cp), thin formations (<9 m), low permeability (< 1 Darcy), and large depths (> 900 m). Non-thermal methods help to increase the recovery by several different mechanisms like reducing the viscosity of the oil, increasing the viscosity of the displacing fluid, altering wettability of the rock, or reducing interfacial tension. The non-thermal methods include polymer flooding, surfactant flooding, water flooding, caustic and emulsion flooding, light hydrocarbon flooding and carbon dioxide flooding. Overall, non-thermal methods have been only marginally successful and not cost-effective for recovering heavy oil (Ahmed et al. 2014).

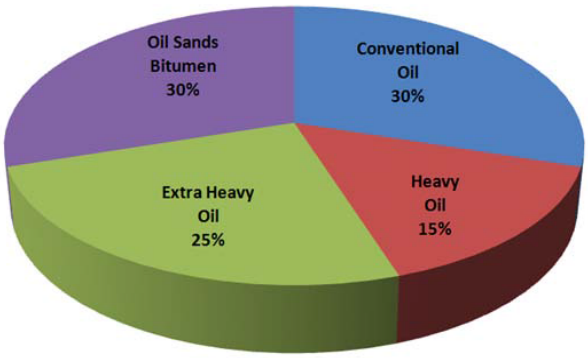

Figure 1: Distribution of the total world oil reserves (Oilfield Review, May 2008).

1.2.2 Thermal Recovery Methods

The two required steps in any bitumen recovery process are:
1) Make the oil sufficiently mobile
2) Provide a driving force to move the mobile oil into a production wellbore. For example, the driving force can be from an imposed pressure difference or gravity drainage, water drive, or solution-gas drive or combinations of them. If one of these steps is not met, then the production would fail.

Thermal techniques increases oil mobility by reducing oil viscosity with heating. For example, Figure 2 shows the viscosity drops of Athabasca bitumen when temperature increases. At initial reservoir conditions (temperature typically between 7 and 15°C), the viscosity is in the millions of centipoise. Above about 200°C, the viscosity is less than 10 cp. To achieve this, many processes, including Cyclic Steam Stimulation (CSS), steam flooding and Steam-Assisted Gravity Drainage, use steam injection into the formation. A certain fraction of the latent and sensible heat of the injected steam is transferred to the oil sands, which heats the bitumen and consequently lowers its viscosity. Other methods for heating the oil include underground combustion, such as in in-situ combustion process, hot water flooding, and electrical heating (Mehrota and Svrcek, 1986).

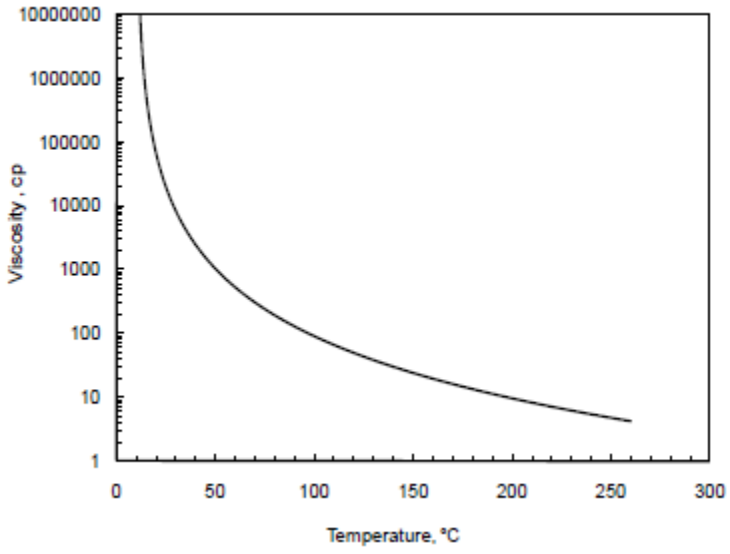

Figure 2: Viscosity of Athabasca bitumen versus temperature (Mehrota and Svrcek, 1986)

1.2.2.1 Steam-Assisted Gravity Drainage and its Variants

Steam-Assisted Gravity Drainage (SAGD) is the main choice to recover bitumen from shallow reservoirs where solution gas content is low and vertical permeability is not significantly impaired. It piloted in Athabasca and Cold Lake reservoirs in Alberta (Komery, Luhning, and Pearce, 1999; Butler, 1997a; Kisman and Yeung, 1995; Ito and Suzuki, 1996; Ito, Hirata, and Ichikawa, 2004; Edmunds and Chhina, 2001; Suggett, Gittins, and Youn, 2000; ERCB website, 2007) and is being used as a commercial technology to recover bitumen in several Athabasca reservoirs (Yee and Spargo, 2001; Farouq Ali, 1997). The pilots demonstrated that SAGD is effective and has the potential for similar scale success in other high viscosity, high permeability oil sands deposits around the world. SAGD has a number of advantages compared with conventional surface mining extraction techniques or other thermal recovery methods. For example, SAGD offers significantly higher production rates per well, lower injection pressures, higher reservoir recovery, steam override elimination, and continuous production.

1.2.2.2 Original SAGD Concept

Roger Butler and his coworkers at Imperial Oil were the first ones who proposed SAGD in the late 1970's (Butler, McNab, and Lo, 1981; Butler and Stephen**,** 1981; Butler, 1985). Figure 3 shows the cross-section of a typical SAGD chamber. In the reservoir, steam flows from the top horizontal injection well into a chamber.

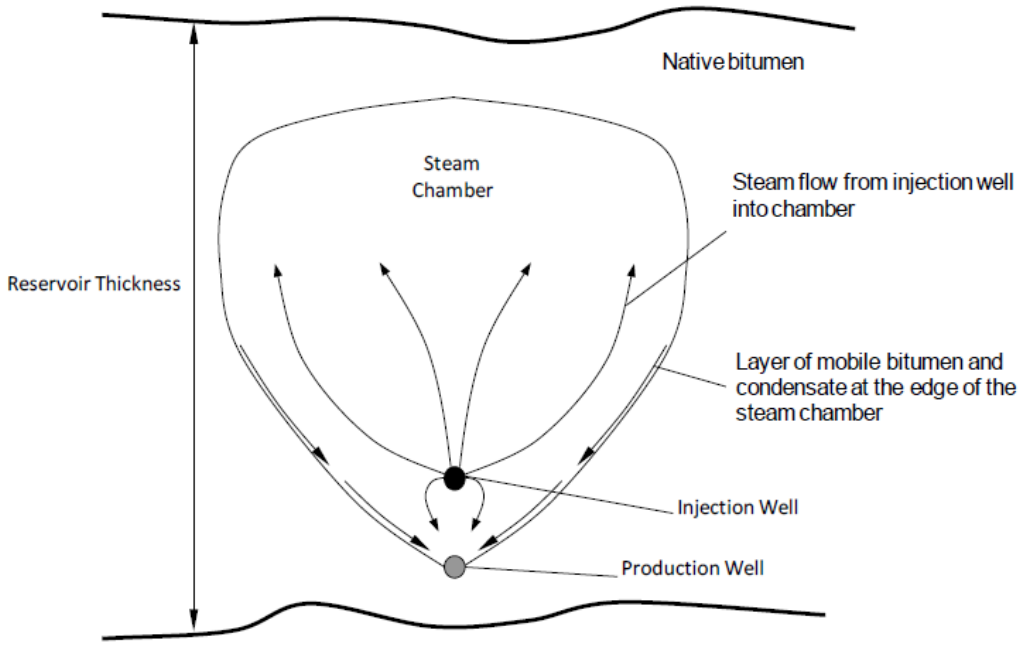

Figure 3: Cross-sectional view of Steam Assisted Gravity Drainage (SAGD).

The production well is typically located a few meters above the base of the oil column whereas the injection well is located between 5 and 10 meters above the production well. A liquid saturation at the base of the chamber surrounds the production well and acts as a steam trap, preventing injected steam from being directly produced from the reservoir. Typically, the lengths of the injection and production wells are between 500 and 1000 m. Since the dominant drive mechanism of SAGD is gravity, relatively shallow reservoirs or ones with low solution gas, such as Athabasca reservoirs, can be produced by SAGD.

The steam flows to the edge of the steam chamber and releases its remaining latent heat to the cool oil sands at the edges. In this work, the 'edge of the chamber' is defined mathematically as the interface beyond which the temperature declines below the saturated steam temperature inside the SAGD chamber. The viscosity of the bitumen drops due to heating effect of steam and the mobilized oil then flows under gravity to the lower horizontal production well. In a SAGD process, the oil layer adjacent to the expanding steam chamber is mobile, and this region is called 'mobile zone' (within the steam chamber, the oil phase is at residual oil saturation

and beyond the heated zone the cold oil phase is practically immobile because of its high viscosity).

1.3 Motivation

The purpose of the work described in this thesis is to develop an analytical model for lateral expansion of steam chamber that accounts for formation and transport of water-in-oil emulsion. . Most of the previous models do not account for thd condensate at the edge of the SAGD. Butler's model overestimates oil production rate due to single-phase assumption, while the proposed model presents more accurate oil flow rate supporting the fact that emulsification effect should be included in the SAGD analysis.

It is assumed that emulsion is generated due to condensation of steam, which is penetrated into the heated bitumen. The oil viscosity is affected by both temperature gradient due to heat conduction and microbubble concentration gradient due to emulsification so the oil flow rate

The proposed mathematical model and its application to field and experimental data help the industry to understand the effect of emulsification on oil mobility during SAGD processes. Based on this understanding, steam chamber growth rate and oil production can be estimated more accurately.

The motivation of this research is to improve our understanding of the underlying physics in SAGD process with recapping the effect of emulsion in the process and filling a critical gap in this area.

1.4 Specific Objectives of this Research

The specific objectives of this research are as follows:

1. Develop an analytical model of SAGD that includes the emulsion effect.

2. Conduct sensitivity analysis with involved parameters such as temperature viscosity and thermal diffusivity parameter.

3. Compare the results yielded by the new models with those given by previous analytical SAGD models and the field data.

1.5 Thesis Outline

Chapter 2, presents a literature review of the analytical models of SAGD process. It highlights the strengths and major shortcomings of the previous analytical models. The recent experiments which emulsions were found both in the porous media and oil produced have been introduced.

In **chapter 3** a detailed overview of the emulsion formation, propagation and coalescence has been explained.

In **chapter 4**, a new model for gravity drainage of mobilized bitumen at the edge of a SAGD steam chamber is derived, that includes emulsion effect. The analytical models derived in this research were compared with 6 set of field data and the system is assumed single phase. The system includes water droplets which are emulsified in the oil phase and are flowing with oil as a single phase.

In **chapter 5**, the multiphase effect is added to the current theory. Emulsion effect is investigated in a two phase flow system which is closer to the real system.

2 Chapter Two: Literature Review

This chapter includes the overview of the existing analytical models of SAGD process. It highlights the strengths and major shortcomings of the previous analytical models. The recent experiments which emulsions were found both in the porous media and oil produced have been introduced.

2.1 Overview

As the oil recovery rate from conventional hydrocarbon resources continues to decline, the role of unconventional heavy oil and bitumen resources become more pronounced. These reserves cannot be produced at effective and economic production rate without assistance of enhanced oil recovery operations, such as Cyclic Steam Stimulation (CSS), Steam Assisted Gravity Drainage (SAGD) or Solvent Aided Processes (SAP) because of their extremely high oil viscosity. Steam injection is a proven thermal technique to be used in heavy, ultra heavy oil and bitumen recovery (Al-Bahlani and Babadagli 2009). Mehrotra and Svrcek (1997) measured the effect of temperature on bitumen viscosity of typical Athabasca bitumen. They observed that bitumen viscosity sharply drops by increasing the temperature.

In SAGD operations, two horizontal wells are drilled in an oil sand deposit. The production well is about five meters below the injection well located at the formation bottom. First, steam is circulated through both injection and production wells. This process is called preheating and the goal is to establish the hot communication. In the next step, steam is injected in the upper well and flows upward in the reservoir. When hot steam contacts cold bitumen, steam transfers its heat to the cold oil. The heated oil and condensate drain towards the lower production well due to gravity. The upper injection well continuously injects steam and the heated oil and condensate are produced through the lower production well. Continuous steam injection forms a steam chamber that develops vertically and horizontally (Canbolat 2002; Butler 2008; Sasaki et al. 1996). Birrell (2001) detected the location of steam chamber by interpreting temperature data. He

specified the regions of constant high temperature as boundaries of the steam chamber.

Butler (1985) developed an analytical gravity drainage model, by combining the flux equation of oil and steam with conduction heat transfer equation, and predicted the oil production rate of a spreading steam chamber in a SAGD process.

Because of the single-phase assumption, his model overestimates the field production data.

Sharma and Gates (2010) extended Butler's model by accounting for the impact of oil saturation and relative permeability to address the discrepancy observed between field data and Butler's model. In both models, the major mechanism of heat transfer at the edge of steam chamber is heat conduction.

The current analytical models do not consider emulsification phenomena which has been observed and reported by several authors. Chung and Butler (1988) studied the production of emulsion under laboratory conditions using a scaled reservoir model to investigate the effect of steam injection geometry on the degree of in-situ emulsification. Ito and Suzuki (1999) simulated the SAGD process and showed that water flow ahead of steam chamber edge and convective heat transfer play significant roles in oil recovery. Sasaki et al. (2001) and (2002) conducted scaled SAGD experiments, and observed that production fluid after breakthrough consists of single-phase condensate and water-in-oil emulsion. The diameter of water droplets was reported to be in the range of 0.01-0.07 mm. Furthermore, pore-level investigations of Mohammadzadeh and Chatzis (2009) demonstrate the simultaneous three-phase flow of steam, condensate, and mobilized oil during a SAGD process. According to flow visualization experiments of Mohammadzadeh and Chatzis (2009), it is evident that water-in-oil emulsion can be formed in-situ during a SAGD process. The water droplet size in their experiments was reported to be in the range of 1.1 to 5μm. They visualized water-in-oil emulsification at the chamber interface caused by local condensation of steam. Noik et al. (2005) observed the existence of residual emulsion in extra heavy oil using Differential Scanning Calorimeter (DSC) during SAGD production. Mohammadzadeh et al. (2010) concluded that temperature gradient between the gaseous mixture and mobile oil phase can affect the extent of emulsification. Azom (2009) studied the

effect of emulsion during SAGD and modeled the emulsion droplets as chemical species. He utilized the features available in CMG simulator in order to model emulsion generation, propagation and coalescence in porous media. He pointed out that transport of these emulsion droplets into the bitumen phase facilitates convective heat transfer resulting in improved oil recovery. Hence the oil rate increases in spite of increase in bitumen viscosity due to emulsion effect. Recently, Ezeuko et al. (2013) conducted a simulation study to investigate the effect of emulsion on SAGD. Their results show that emulsification increases bitumen mobility and therefore decreases cSOR. More recently, Ezeuko et al (2013) numerically simulated the effect of emulsion in a SAGD process and compared the simulation results with the experimental results. They concluded that in-situ emulsification may play a vital role within the reservoir during SAGD, increasing bitumen mobility and thereby decreasing cumulative steam/oil ratio.

Reverse emulsion can also occur during SAGD production. Reverse emulsion is produced by emulsification of oil in a continuous water phase. As a general rule, the phase with the smaller volume fraction is the dispersed phase and the other phase will be the continuous phase. When both phases are at the same magnitude, other factors will determine type of emulsion formed (Kokal 2005). Water-in-oil emulsion could invert to oil-in-water emulsion typically when water volume fraction is greater than 80%. Furthermore, steam quality may play an important role in emulsification (Ezeuko et al.2013; Kokal 2005). Azom (2013) states water-in-oil emulsion occurs when steam quality is high.

In this thesis, we added the effect of emulsion into Butler's model to address overestimation of oil flow rate. The proposed mathematical model and its application to field and experimental data help the industry to understand the effect of emulsification on oil mobility during SAGD processes. Based on this understanding, steam chamber growth rate and oil production can be estimated more accurately.

2.2 Analytical Modelling of Steam-Assisted Gravity Drainage (SAGD)

2.2.1 Butler Single Phase Model

Butler et al. (1979) presented the first paper on SAGD at the Oil sands Symposium in Jasper, Canada. The key physics of SAGD are relatively well and simply described the oil drainage rate from first principles (Butler et al. 1981; Butler and Stephens, 1981; Butler, 1985; Ferguson and Butler, 1988; Reis, 1992, 1993; Butler, 1997a; Akin, 2005). Butler et al. (1981, 1985) analysis underlies all SAGD theories that have been published till today (Ferguson and Butler, 1988; Reis, 1992, 1993; Akin, 2005). He developed a gravity drainage model, with a fundamental assumption that the only heat transfer mechanism at the edge of steam chamber is conduction. Also, the temperature ahead of the interface is assumed to have a quasi-steady state distribution in the direction normal to the chamber edge, which means that the time-scale of heat transfer is similar to the time-scale of the interface advance. Hence, the temperature profile is given by

$$T^* = \frac{T - T_R}{T_s - T_R} = e^{(-U\varepsilon/\alpha)} \quad (1)$$

Where T^*, T_R, and T_s are dimensionless temperature, initial reservoir temperature and steam temperature, respectively. U is the advance velocity of steam chamber edge, which is normal to the interface. ε is the distance away from the chamber edge, with a coordinate normal to the interface. α is the thermal diffusivity given by $\alpha = k_{TH}/\rho C_P$, where k_{TH}, ρ, and C_P are the thermal conductivity, rock density, and specific heat capacity of the formation, respectively. In simple, α controls the ability of a material to conduct thermal energy. When α is higher the heat transfer is more efficient.

The kinematic viscosity as a function of temperature is assumed to be

$$\frac{\nu_s}{\nu_o} = \left(\frac{T - T_R}{T_s - T_R}\right)^m \quad (2)$$

Where ϑ_s and ϑ_o are kinematic oil viscosity at steam temperature (T_s) and reservoir temperature (T_R), respectively. m is a temperature viscosity parameter. For heavy crude oil and bitumen, the value of m is typically between 3 and 4 (Butler, 1985).

Substituting Eq. 1 into Darcy equation and using the relationship between advance velocity and the system geometry, oil flow rate becomes

$$Q = 2\,L\sqrt{\frac{2\,\emptyset\,\Delta S_o\,k\,g\,\alpha\,h}{m\,\nu_s}} \tag{3}$$

where q is the volumetric bitumen production rate, L is the length of the production well, k, α, φ, ΔS_o, are the permeability, thermal diffusivity, porosity, and mobile oil saturation range of the reservoir, respectively. Detail of the calculations is shown in appendix A. $\emptyset$, ΔS_o , k , g and h are porosity, oil saturation difference, permeability, gravitational acceleration and reservoir thickness. As Butler analyzed the oil flow in a 2-D model, the flow rate, Q, has a unit of m^2/s. The reservoir is assumed to be laterally infinite and there is no dissolved gas in the oil phase.

2.2.2 Other Variants of Butler's Models

The original theory was revised by Butler and Stephen (1981) to model the chamber shape such that it remained attached to the production well. The oil production rate predicted by this revised model, referred to as the "Tandrain" model, is given by

$$q = 2L\sqrt{\frac{1.5kg\alpha\varphi h\Delta S_o}{m\nu_s}} \tag{4}$$

Ferguson and Butler (1988) reported a procedure to investigate the impact of variable steam injection rates and pressure on SAGD. Their improved the original SAGD theory because it could handle varying steam pressures. However, the resulting theory was developed numerically and required the solution of a complex differential equation that approximated heat transfer at the boundary of the steam chamber as a constant temperature boundary at the edge of the chamber.

Reis (1992) derived a SAGD theory similar to Butler's (1985) theory for horizontal wells. He assumed the steam chamber shape as an inverted triangle. This shape was in Hele-Shaw and sandpack laboratory models (Chung and Butler, 1988) but

thermocouple data (EnCana report, 2007; CNRL report, 2007; ConocoPhillips report, 2008) from field operations and detailed simulation studies (Ito, Hirata, and Ichikawa, 2001b; Gates, Kenny, Hernandez-Hdez, and Bunio, 2005) suggest that the steam chamber is more elliptical. Reis (1992) derived a similar theory for steam-based gravity drainage in radial geometry around vertical wells. He assumed that the steam chamber is an inverted cone and used material and energy balance equations to determine a steam to oil ratio. Reis used his theory to demonstrate that vertical well SAGD may have potential as a bitumen recovery process. The oil drainage rate predicted by Reis for a linear geometry is given by

$$q = 2L\sqrt{\frac{kg\alpha\varphi h\Delta S_o}{2\alpha_R m v_s}} \tag{5}$$

Where, a_R is an empirical constant equal to 0.4. Reis (1992, 1993) showed that Butler's model overpredicts the oil production rates compared to the experimental results. However, his model did not predict production during the rise of the chamber.

SAGD is a multi-physics process involving simultaneous mass and heat transport, with significant thermal, geomechanical, and interfacial effects. Butler's model has been extended by several researchers to account for such effects. Akin (2005) developed a mathematical model for gravity drainage during steam injection that accounted for steam distillation and asphaltene deposition eddects in a linear geometry where the steam chamber is assumed to be an inverted triangle shape. His analysis showed that in late times, steam-distillation and asphaltene deposition are the controlling parameters of the process rather than steam chamber size and lateral heat transfer. He implemented the effects of temperature, pressure and asphaltene-content on the viscosity of the drained oil by using a compositional viscosity model. Irani and Cokar (2014) developed an approach to incorporate temperature-dependant thermal conductivity into a SAGD analytical model. Azad and Chalaturnyk (2010 and 2012) proposed a circular geometry formulation to model the SAGD process. Cokar et al. (2013) derived a formula that accounts for thermogeomechanical effects at the edge of the steam chamber.

Wei et al (2014) developed a new model which considers the time-dependent overburden heat losses. Heidari et al. (2009) developed a model to study effects of drainage and permeability on production rate in a SAGD process. Their model introduces the dilation effects arising from thermal expansion into the analytical model for SAGD oil production. Azom et al. (2013) studied interfacial phenomena during the SAGD process, and concluded that Butler's and Sharma and Gates's solutions are respectively more accurate at relatively low and high values of Marangoni number. Rabiei et al. (2014) developed an unsteady-state semi-analytical model to predict the oil flow rate in a solvent-assisted SAGD process.

2.2.3 Sharma and Gates' Multiphase Model

Butler's derivation assumes a single phase flow and does not account for relative permeability effect at the interface. By extending Butler's theory, Sharma and Gates (2010) developed a multiphase SAGD model, with an assumption that oil saturation linearly changes with respect to temperature ahead of the steam chamber, ranging from the residual oil saturation at the edge of steam chamber to the initial reservoir oil saturation .Thus, the oil saturation profile is given by

$$S_o = S_{or} + (S_{io} - S_{or})(1 - T^*) \quad (6)$$

Where S_{or} and S_{io} are residual and initial oil saturation, respectively.

The relative permeability of oil depends on the oil saturation, which varies with the distance beyond the steam chamber edge. It can be determined from lab-based relative permeability models such as (Brook and Corey, 1964)

$$k_{row} = k_{rocw}(1 - S_{wD})^a \quad (7)$$

The exponent "a" is a Corey coefficient, which controls the curvature of the oil relative permeability curve. k_{ro}, k_{rocw} and S_{wD} are relative permeability of oil phase with respect to water, relative permeability of oil phase at irreducible water saturation, and the normalized water saturation, respectively. The normalized water saturation is defined as

$$S_{wD} = \frac{S_w - S_{wc}}{1 - S_{wc} - S_{or}} \tag{8}$$

Where S_{wc} and S_{or} are connate water saturation and residual oil saturation, respectively.

The oil flow rate equation developed by Sharma and Gates is finally given by

$$Q = 2L\sqrt{\frac{2\,\alpha\,k\,k_{rocw}\,g\,\emptyset\,\Delta S_o\,h\,\Gamma(m+1)\Gamma(a+1)}{\nu_s\Gamma(m+a+1)}} \tag{9}$$

Γ is gamma function.
The difference between this volumetric flow rate equation and Butler's model is the following term, which accounts for the multiphase effects. The detail of the calculations can be found elsewhere (Sharma and Gates, 2010).

$$\sqrt{\frac{\Gamma(m+1)\Gamma(a+1)}{\Gamma(m+a+1)}}$$

2.2.4 Energy Balance

In this section the steam oil ratio is determined by energy balance (Murtaza. et al. 2014). Based on Butler (1987) there are three types of heat which is transferred to the system. The heat transferred to rock, residual oil and connate water within the finger is H_f. The heat transferred to the oil stream at the edge of steam chamber, H_o. The heat conducted to the oil saturated reservoir, H_r.

$$H_f = \rho_c C_c V(T_s - T_r)x_i$$

$$H_o = V\emptyset\Delta S_o(T_m - T_r)x_i[\rho_o C_o]$$

Where T_m is temperature of heated bitumen, $\rho_c C_c$ is volumetric heat capacity of steam chamber excluding condensate, x_i is interface position of steam and drainage flow, A_{m1} is constant.

$$H_r = V\{\rho_c C_c x_i(T_s - T_r) + \frac{A_{m1}}{2}x_i[\emptyset\Delta S_o[\rho_o C_o + \rho_w C_w](T_s - T_r)]\}$$

Where, $T_m = \frac{A_{m1}}{2}(T_s - T_r) + T_r$

$$A_{m1} = \frac{m+1}{m+2} + \frac{\left(\frac{\pi}{12}\frac{\pi^2}{160} + \frac{\pi^3}{2688}\frac{\pi^4}{55296} + \frac{\pi^5}{1351680} - \frac{\pi^6}{38338560}\right)^{m+2} - 1}{\left(\frac{\pi}{12}\frac{\pi^2}{160} + \frac{\pi^3}{2688}\frac{\pi^3}{55296} + \frac{\pi^5}{1351680} - \frac{\pi^6}{38338560}\right)^{m+1} - 1}$$

The weighted steam/oil ratio is given by:

$$\mathrm{Rg}' = \frac{(T_s - T_r)}{\Delta S_o \lambda \emptyset \rho_o}\{\rho_c C_c + \frac{A_{m1}}{2}\emptyset \Delta S_o[\rho_o C_o + \rho_w C_w]\}$$

3 Chapter 3: Emulsions in SAGD

A detailed overview of the emulsion characteristics and important factors on emulsion stability has been explained in this chapter.

3.1 Definitions

Emulsification can occur in most of the oil production and processing like inside the reservoir, wellbore, wellheads and transportation pipelines even in the storages. An oil emulsion is a dispersion of water droplets in oil. Emulsions can be classified into three groups:

- Water in oil emulsions (W/O)
- Oil in water emulsions (O/W)
- Complex emulsions

The W/O emulsion includes water droplets in a continuous oil phase and the O/W emulsion includes oil droplets in a continuous water phase. Complex emulsions include tiny droplets suspended in bigger droplets that are suspended in a continuous water phase. As a rule of thumb, the dispersed phase is the one in the mixture which the volume fraction is smaller compared with the other one (continuous phase). In case that the phase volume ratio is close to 1, other factors will determine the type of emulsion formed. (Kokal 2005, Farah et al. 2005)

3.2 Emulsion Characteristics

3.2.1 Droplet Size

Produced emulsions have droplet diameters 0.1 μm – 50 μm. Emulsion droplet size distribution depends on number of factors like IFT, nature of emulsifying agents and presence of solids. Droplet size distribution may be a factor to determine emulsion stability. The smaller the average size of dispersed water droplets the longer the residence time required (Kokal 2005).

3.2.2 Viscosity

Due to non-Newtonian behavior of emulsions caused by droplet crowding, emulsion viscosity is higher than either oil or water viscosity. As a certain value of water, emulsions would behave as shear thinning or pseudoplastic fluids, as shear rate increases the viscosity decreases (Noik et al. 2005). The viscosity data shown in Figure 4 indicates that emulsions exhibit Newtonian behavior up to a water content of 30 % (this is indicated by constant values of viscosity for all rates or a slope of zero)(Kokal 2005). For water cuts above 30 % the slope would deviate from zero showing the non-Newtonian behavior. Kokal (2005) observed in the Saudi Arabian crude emulsions that water cut exceeds than 80% W/O emulsion inverts to O/W emulsion. The viscosity of emulsion is affected by number of parameters like:

- Temperature
- Amount of dispersed water
- Droplet size and distribution
- Oil and water viscosity
- Amount of solid presents
- Rate of shear or shearing force
- Temperature viscosity parameter
- Thermal diffusivity parameter

Among them temperature and amount of dispersed water and rate of shear have the main effect and others have minor effect on the viscosity (Broughton and Squires 1938).

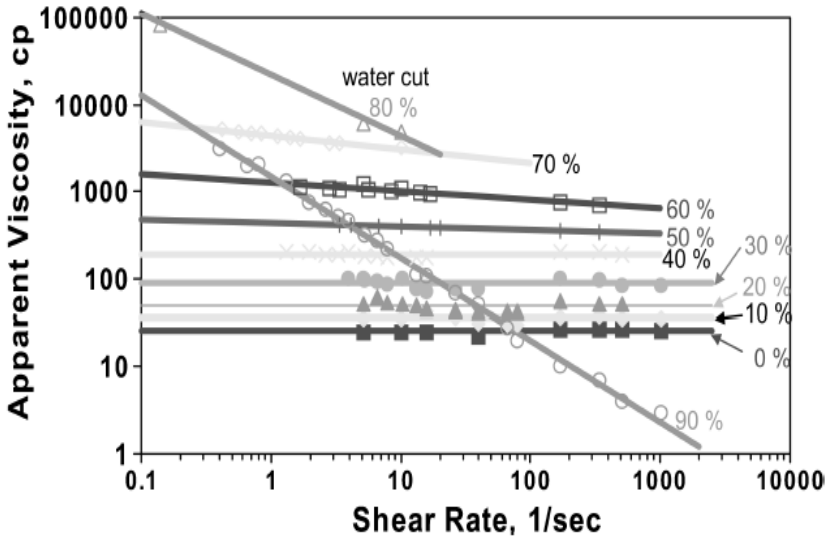

Figure 4: Viscosities of very tight emulsions at 125° F. (Kokal 2005).

From the pore-scale schematic in Figure 5, due to emulsification effect at the water-oil interface, a fraction of water flows with the continuous oleic phase in the form of dispersed droplet, instead of flowing as a separate continuous phase. Emulsification phenomenon at the interface during the advance of steam chamber is not considered in previous analytical models. Several authors reported formation of emulsion during SAGD production in the reservoir, wellbore, wellhead, and transportation pipelines (Kokal 2005, Ronningsen 1995).

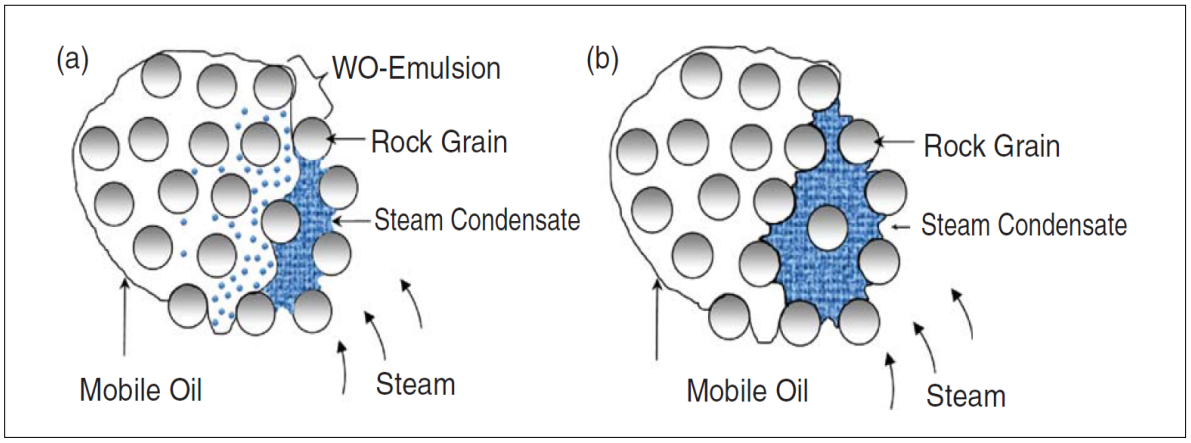

Figure 5: Pore-scale illustration of fluid occupancies (water, oil) at the edge of steam chamber: (a) WO emulsion SAGD, (b) traditional SAGD (Ezeuko et al. 2013).

The viscosity of a liquid which small solid spheres are dispersed in it, studies by Einstein in theoretical hydrodynamics. Taylor (1932) stated that Einstein analysis may be extended to include the liquid droplets.

Based on Taylor's empirical relationship (Taylor 1932),

$$\frac{\mu_{em}}{\mu} = 1 + \left[2.5\left(\frac{\tau + 0.4}{\tau + 1}\right)\right] x \quad (1)$$

This equation shows that the viscosity of emulsion increases by increasing the volume fraction of dispersed water at constant temperature. Here, τ is the ratio between the viscosity water droplets and continuous oil phase; $\mu_{em}\ and\ \mu$ are emulsion viscosity and continuous oil phase viscosity, respectively; and x is the dispersed phase volume fraction. Taylor's equation is applicable under the following conditions:

a) Low concentration of the dispersed phase (Farah et al. 2005). Increasing the dispersed phase concentration increases the chance for interactions among and deformation of the original spherical droplets. Based on the experiments, when the water saturation exceeds 80 % the system inverts to oil-in-water emulsion.

b) The radii of dispersed phase droplets do not exceed a certain critical radius (Broughton and Squires 1938).

c) Droplets of the dispersed phase should not be deformed from the original spherical shape (Farah et al. 2005).

d) The tangential stress parallel to the surface is continuous at the surface of the droplet, so any film existing between the two liquids only transmits tangential stress from one fluid to the other one.

In Taylor's relationship, viscosity is a function of dispersed phase volume fraction. However, there are several other correlations describing viscosity as a function of temperature and dispersed phase volume fraction (Farah et al. 2005, Broughton and Squires 1938, Pal 1998, Krieger and Dougherty 1959). Here, we assume that when $S_w < 0.6$, water droplets do not deform and coalesce. Furthermore, we assume that the radius of the dispersed droplets does not exceed the critical value.

3.2.3 Color and appearance

The color of the emulsion can vary widely depending on:

- Oil/water content
- Characteristics of the oil and water

The common colors of emulsions are dark reddish brown, gray, or blackish brown; however, any color can occur depending on the type of oil and water at a particular facility. Emulsion brightness is sometimes used to characterize an emulsion. An emulsion generally looks murky and opaque because of light scattering at the oil/water interface. When an emulsion has small diameter droplets (large surface area), it has a light color. When an emulsion has large diameter droplets (low total interfacial surface area), it generally looks dark and less bright. Understanding the characteristics of an emulsion by visual observation is an art that improves with experience (Sarbar and Wingrove 1997).

3.3 Emulsion Stability

Emulsifiers (surface active agents or surfactants) that concentrate at the oil/water interface and form the interfacial films would stabilize the emulsions. They lead to reduction in interfacial tension and emulsification of droplets as well. Emulsifiers have higher boiling point fractions such as asphaltenes, resins, organic acids and bases. There are natural and chemical emulsifiers. Chemical ones include surfactants that may be injected into formation or wellbore (drilling fluids, stimulators). Fine solids may play as an emulsifier. The effectiveness of them may depend on some factors like particle size, particles interaction and wettability of the particles.

From thermodynamic point of view an emulsion is an unstable system. It is because each liquid/liquid system tends to reduce the interfacial area and energy by separation. Emulsions are classified based on their kinematic stability to three groups.

Loose emulsions: separate in a few minutes.
Medium emulsions: separate in 10 minutes or more.
Tight emulsions: separate partially in hours or days.

Interfacial films play an important role in emulsion formation and stability. The films are formed due to adsorption of polar and high weight molecules which are active at the interface. They would reduce the IFT and increase the interfacial viscosity at the same time. The strength of films is a function of temperature, pH of water and oil type (polar molecules). The films can be rigid (solid) or mobile (liquid).
The rigid films have very high interfacial viscosity like an insoluble skin. They provide structural barrier and help to increase emulsion stability. Mobile films are characterized by low interfacial viscosity. They are less stable. Surfactants can modify the stability of films and eventually the emulsions (Poindexter et al. 2006).

The important factors affecting emulsion stability include the following:

3.3.1 Steam Quality

Chung and Butler (1989) reported from a 2D experimental model no significant difference on emulsification with wet or dry steam. They attributed that to the interfacial activities and the heating mechanism being the same at the steam front. The comparison was done on a low pressure injection, and they did not report any high pressure. Their observation supports the fact that steam quality is controlled by reservoir temperature and pressure. Although we can control the quality of injected steam to keep it as high as possible, it drops as it flows through the reservoir. Although Gates and Chakrabarty (2005) stated that the quality of the injected steam should be as high as possible at the sandface because any condensate in the injected fluids falls under gravity from the injector towards the producer and does not deliver a significant amount of heat to the oil sand.

3.3.2 Temperature

Temperature affects the physical properties of oil, water and interfacial films surrounding the water droplets that give the emulsions their stability. Waxes can dissolve in crude oil when temperature increases. Waxes are the main constituents of the interfacial films surroundings the water droplets. Hence dissolving of waxes

into the crude oil reduces the chances of water droplets to form as an emulsion. Temperature also increases the thermal energy of the droplets and hence increases the frequency of droplet collisions. Gradual destabilization of the crude oil/water interfacial films is another result of increasing temperature. Increasing temperature causes the reduction in interfacial viscosity of the interfacial films which results in the instability of emulsion. Highly viscous interfacial films retard the rate of oil-film drainage providing a mechanical barrier to coalescence (Kokal 2005). However, decreasing viscosity of the system causes the higher rate of drainage at the edge, which makes the size of the water droplets smaller and more stable and suitable for making emulsion.

3.3.3 Initial Water Saturation

Chung and Butler (1989) noticed a higher water in oil emulsion when S_{wi} = 0% than S_{wi} = 12.5%. They commented that there is less tendency for water to condense as droplets on the surface of oil when enough connate water is available.

As the droplets of water condense on oil, they become "buried" because of the spreading characteristics of oil. It is worth mentioning that Sasaki et al. (2002) observed this process in a microscopic visualization experiment.

m*:** In crude samples with higher value of m, the concentration of naturally occurring emulsifiers like higher boiling point fraction in oil is higher. Hence the probability of forming emulsions may increase when ***m increases.

α: For higher value of α which means the heat will diffuse more quickly, we expect to have less emulsion. Higher rate of heat diffusion results in sharp viscosity drop, so the drainage rate will be faster. The chance of water droplet coalescence may be more than having dispersed water droplets as emulsions.

3.3.4 Rate of Steam Injection

Higher injection rate can make a faster drainage rate at the edge and may enhance droplet coalescence. Hence higher injection rate can result into less emulsification.

3.3.5 Oil Production Rate

In higher oil production rate, water droplets may have more chance to coalescence so even when there are some emulsions in the system they would disappear.

3.3.6 Pressure

Chung and Butler (1989) conducted high pressure experiments on the steam assisted gravity drainage process using a scaled physical model. The results showed that the pressure variation of steam injection does not have significant effect on the emulsified water ratio. It is well-known that naturally occurring emulsifiers are concentrated in heavy fraction in crude oil such as asphaltenes, resins and oil-soluble organic acids (Kokal 2005). These components are the main constituents of the interfacial films surrounding the water droplets that give the emulsions their stability. Therefore, it can be interpret that the steam injection pressure does not significantly affect the emulsion stability.

3.3.7 pH

For oil-water systems, there exists an optimum pH range for which the interfacial film exhibits minimum emulsion stabilizing. The optimum pH for maximum emulsion stability depends on both the oil and water composition. (Kokal 2005)

3.3.8 Droplet Size

When the size of the water droplet is smaller forming emulsion is easier. Generally the emulsions that have smaller-sized droplets will be more stable. (Kokal 2005)

3.3.9 Heavy Fraction in Crude Oil

Asphaltenes, resins and oil soluble organic acids (e.g., carboxylic and naphthenic acids) are the main part of the interfacial film. They reside at the oil- water interface because of their surface active properties. The accumulation of them at the interface results in the formation of a rigid film. (Kokal 2005). There are still debates on the resins and waxes effect on emulsion stability in the literature while the effect of asphaltenes on increasing emulsion stability has been approved. Crude oil that has low cloud point have greater tendancy to form stable and tight emulsions.

3.3.10 Solid particles

Fine solid particles present in the crude oil are capable to stabilize the emulsion. They diffuse to the oil-water interface where they form rigid structure to form emulsion and help to inhibit of emulsion coalescence. If the solid particles at the interface are charged they may increase the stability of the emulsion. To act as a stabilizer the size of the solids should be smaller than the size of the emulsions. When the solids are oil wet like asphaltenes and waxes a water in oil emulsion will result, because the particles partition into oil phase and will prevent the coalescence of water droplets. Similarly, water wet solid like $CaCO_3$ and $CaSO_4$ (clays and sands) will stabilize oil in water emulsion.(Kokal 2005)

3.3.11 Counter current flow

Counter current flow increases the chance of emulsion formation. Chung and Butler (1989) observed much higher water/oil emulsion content in the produced fluid when the steam chamber was rising in the experiment with bottom steam injection than with injection at the top.

3.4 Thermodynamics of Emulsion

As mentioned previously in this chapter emulsions are thermodynamically unstable. Emulsification is an exothermic process and can be described in two steps. Step 1 is transferring of water micro bubbles across the bitumen interface (Equation 2) the enthalpy released is the heat which is generated and transferred to bitumen. Step 2 is the process of encapsulation of emulsions into bitumen(Equation 3). The reactions are first order and dependent on the emulsion concentration. The stoichiometric constants A, B, X and Y will be determined by experimental analysis. (Ezeuko et al. 2013)

$$X(H_2O) \longrightarrow Y(\text{Emulsion}) \qquad [\Delta H_{\text{Emulsification}}] \qquad (2)$$

$$A(\text{Emulsion}) + B(\text{Bitumen}) \longrightarrow D\,(WO_{\text{Emulsion}}) \qquad (3)$$

Kumar et al (2012) studied effect of in situ emulsion in heavy oil recovery. Since the key problem in heavy oil is sweep efficiency and flow rate. They proposed using Alkaline surfactant flooding can form W/O emulsion based on the solubility of the surfactant. If the O/W emulsion formed the viscosity would be lower than the original oil. Bypassed oil can be emulsified at the surface of water fingered mobilized and produced at relatively low pressure gradient.

4 Chapter 4: Single Phase Analytical Modeling of SAGD

The purpose of this chapter is to develop a new gravity drainage model of mobilized bitumen at the edge of steam chamber which includes emulsion effect in in a single phase system. Considering that several SAGD experiments reported water-in-oil emulsion, we restrict water fraction evaluated in our model to be less than 80%. We develop a new analytical oil drainage model by extending Butler's (1985) and Sharma and Gates' (2010) models to account for water-in-oil emulsification effect. The oil flow rate from the new theory is calculated and compared with other analytical SAGD theories, and with the production data from several existing SAGD operations, as well as experimental data. Overestimation of oil flow rate calculated by Butler's model is clearly predictable. Sharma and Gates tried to address overestimation problem of Butler's model by considering multiphase effects and adding relative permeability into Butler's model.

Assumptions of the model are as follow:

1. Heat transfer ahead of the chamber edge is only by conduction.
2. All the water is emulsified in the system.
3. Porous medium is homogeneous (constant porosity and permeability).
4. Heat losses are neglected.
5. Density is dependent on temperature.
6. Steam chamber that has reached the maximum height, h, and is expanding at a constant velocity U, in the direction perpendicular to the chamber walls.
7. Reservoir oil does not have any solution gas.
8. Heat transfer and mass transfer is directed normal to the edge of the chamber.

4.1 Proposed Theory

Figure 6 shows a conceptual model of a differential element at the edge of the steam chamber. As the distance beyond the steam chamber edge increases, the temperature decreases from steam temperature to reservoir temperature. In this

model, all of the water in the formation is assumed to be emulsified in the oil phase. Emulsion concentration decreases from a maximum value at the chamber interface to zero far from the interface. Water saturation is maximum at the chamber edge ($\varepsilon = 0$) and it equals to the connate water saturation far enough from the edge.

Emulsion at the steam chamber interface is a system of immiscible fluids, with water droplets as the dispersed phase, and oil as the continuous phase. Therefore, Taylor equation becomes

$$\frac{\mu_{em}}{\mu_o} = 1 + \left[2.5\left(\frac{\frac{\mu_w}{\mu_o} + 0.4}{\frac{\mu_w}{\mu_o} + 1}\right)\right] S_w \qquad (1)$$

There are several other equations for calculating emulsion viscosity at certain conditions. At high concentration of dispersed phase, the droplets can interact and deform from the spherical shape. Yaron and Gal-Or (1972) and Choi and Schowater (1975) suggested correction factors for Taylor equation to take into account the deformation of droplets. Both models describe the viscosity variation as a function of dispersed phase volume fraction but not the temperature. In our model which we used Taylor equation, we consider the effect of temperature with using the relation of water saturation with distance and temperature. Several authors proposed correlation for the viscosity of W/O emulsion as a function of temperature and dispersed phase volume fraction like Ronnigsen (1995) Richardson (1950) and Walther (1931).

In our theory, we assume that all the water is emulsified in the oil phase. This assumption is in agreement with the experimental study conducted by Noik et al. (2005) to characterize the water-in-oil emulsion produced by SAGD operation. Based on their results, when the water cut is about 40%, water is totally emulsified. They also mentioned that a threshold energy exists above which the oil-water system tends to be totally emulsified.

By solving Eq. 1, we have

$$\mu_{em} = \frac{\mu_w + \mu_o + (2.5\mu_w + \mu_o)(S_w)}{\left(\frac{\mu_w}{\mu_o} + 1\right)} \qquad (2)$$

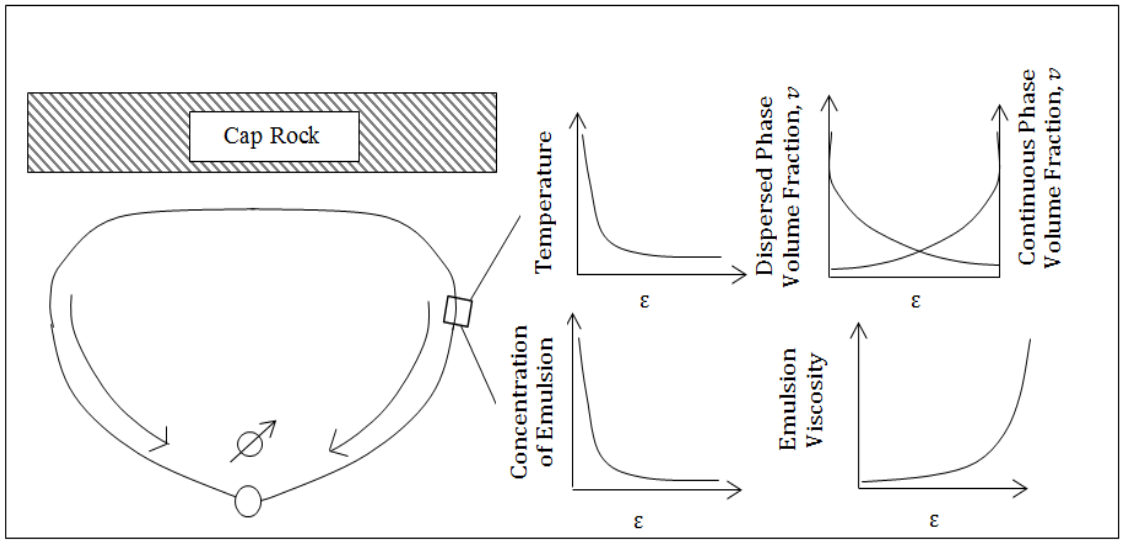

Figure 6: Schematic illustration of temperature, dispersed and continuous phase volume fraction, emulsion concentration and emulsion viscosity with respect to the distance beyond the steam chamber edge (ε).

We also assume that oil saturation is a linear function of temperature ahead of the interface, with an assumption that conductive heat transfer dominates beyond the steam chamber edge:

$$S_w = 1 - S_o = (1 - S_{or}) - (S_{io} - S_{or})(1 - T^*) = (1 - S_{or}) - (S_{io} - S_{or})\left(1 - e^{\left(-\frac{U\varepsilon}{\alpha}\right)}\right) \quad (3)$$

This relationship, which was first proposed by Sharma and Gates (2010), requires the assumption of similar length scales for capillary diffusion and thermal diffusion. According to Azom et el. (2013), this assumption can hardly be justified for a capillary dominated flow at the edge of the steam chamber. However, in the presence of emulsions, the length scale of saturation advection can be assumed to be similar to that of thermal convection. It should be noted that emulsions are generated primarily by condensation of penetrated steam (Mohammadzadeh and Chatzis (2009)), and therefore, heat transport ahead of the steam chamber is controlled by both conduction and convention mechanisms (Azom and Srinivasan (2009)).

Eventually, water saturation becomes a function of distance (ε) beyond the steam chamber interface. Substituting $\frac{1}{\mu_o} = \frac{\delta^{-m}}{\mu_s}$ and Eq.3 into Eq.2, the dynamic emulsion viscosity as a function of distance beyond the steam chamber interface is given by

$$\mu_{em} = \frac{\mu_w + \frac{\mu_s}{\delta^{-m}} + \left(2.5\mu_w + \frac{\mu_s}{\delta^{-m}}\right)[(1 - S_{or}) - (S_{io} - S_{or})(1 - \delta^{-1})]}{\left(\frac{\mu_w \delta^{-m}}{\mu_s} + 1\right)} \quad (4)$$

Where $\boldsymbol{\delta = e^{\left(\frac{U\varepsilon}{\alpha}\right)}}$

Therefore, emulsion mobility defined by $\lambda_{oil} = \frac{k}{\rho_{em}\nu_{em}} = \frac{k}{\mu_{em}}$ is given by

$$\lambda_{oil} = \frac{k\left(\frac{\mu_w \delta^{-m}}{\mu_s} + 1\right)}{\mu_w + \mu_s \delta^m + (2.5\mu_w + \mu_s \delta^m)[(1 - S_{or}) - (S_{io} - S_{or})(1 - \delta^{-1})]} \quad (5)$$

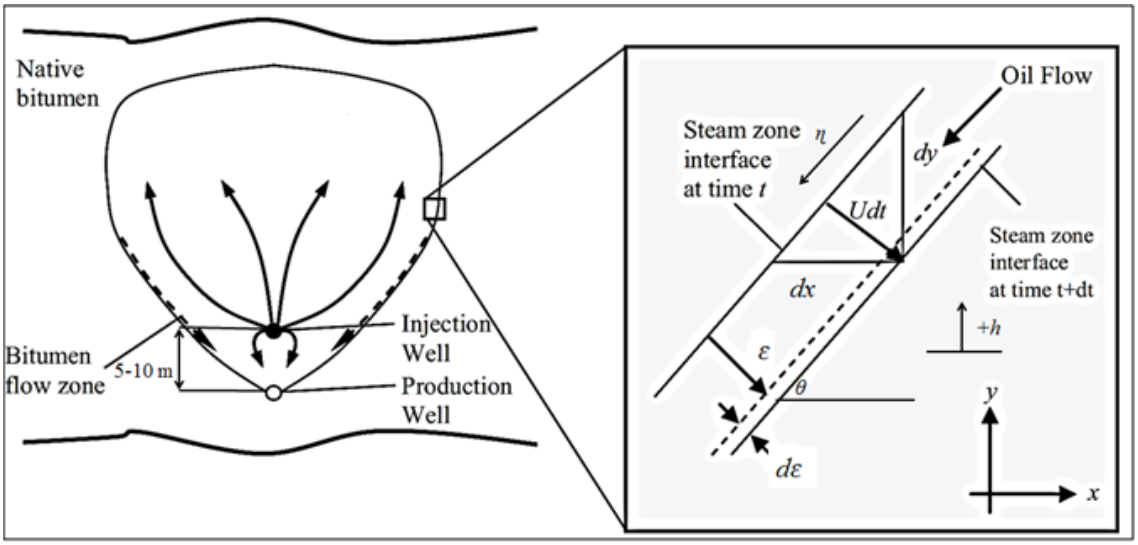

Figure 7: Cross sectional view of a typical SAGD process and expanded view of a differential element at the edge of steam chamber (modified from Sharma and Gates 2010).

4.1.1 Total oil flow rate

Here, we follow Butler's approach (Butler et al. 1981) to develop an expression for the total oil flow rate by combining Darcy's and mass conservation laws.

4.1.2 Darcy's law

Integration of differential Darcy's law equation for emulsion flow results in:

$$q_o = k\,S_o\,g\sin\theta\int_0^{\infty}\frac{d\varepsilon}{\nu_{em}} = k\,S_o\,g\sin\theta\int_0^{\infty}\frac{\rho_{em}}{\mu_{em}}\,d\varepsilon \tag{6}$$

Let $A = {}^{U}/_{\alpha}$, $x = A\varepsilon$, $dx = Ad\varepsilon$, $d\varepsilon = \frac{1}{A}dx$:

$$q_o = \frac{k\,g\sin\theta}{A}\int_0^{\infty}\frac{S_o(a\frac{\mu_w}{\mu_s}e^{-(m+1)x} + ae^{-x} + \rho_o\frac{\mu_w}{\mu_s}e^{-mx} + \rho_o)}{\mu_w + \mu_s e^{mx} + 2.5(S_{io} - S_{or})\mu_w e^{-x} + \mu_s(S_{io} - S_{or})e^{(m-1)x}}dx \tag{7}$$

Let $\delta = e^x$, $d\delta = e^x dx$, therefore, $dx = e^{-x}d\delta = \frac{1}{\delta}d\delta$

$$q_o = \frac{k\,g\sin\theta}{\mu_s A}\int_1^{\infty}\frac{S_o\left(\frac{a\mu_w}{\delta^{m+1}} + \frac{a\mu_s}{\delta} + \frac{\rho_o\mu_w}{\delta^m} + \rho_o\mu_s\right)\frac{1}{\delta}}{\mu_w + \mu_s\delta^m + \frac{2.5(S_{io} - S_{or})\mu_w}{\delta} + \mu_s(S_{io} - S_{or})\delta^{m-1}}d\delta \tag{8}$$

$$q_o = \frac{k\,g\sin\theta}{\mu_s\,A}\int_1^{\infty}\frac{S_o\left(\frac{a\mu_w}{\delta^{m+1}} + \frac{a\mu_s}{\delta} + \frac{\rho_o\mu_w}{\delta^m} + \rho_o\mu_s\right)}{\mu_w\delta + \mu_s\delta^{m+1} + 2.5(S_{io} - S_{or})\mu_w + \mu_s(S_{io} - S_{or})\delta^m}d\delta \tag{9}$$

Substituting $A = {}^{U}/_{\alpha}$, gives:

$$q_o = \frac{k\,g\sin\theta}{\mu_S\,U}\int_1^{\infty}\frac{S_o\left(\frac{a\mu_w}{\delta^{m+1}} + \frac{a\mu_s}{\delta} + \frac{\rho_o\mu_w}{\delta^m} + \rho_o\mu_s\right)}{\mu_w\delta + \mu_s\delta^{m+1} + 2.5(S_{io} - S_{or})\mu_w + \mu_s(S_{io} - S_{or})\delta^m}d\delta \tag{10}$$

Here it is assumed that steam density is significantly lower than emulsion density. g is the acceleration due to gravity, and θ is the local inclination angle for the steam chamber interface. Eq. 10 gives the relative flow rate of oil per unit well length, assuming single-phase flow of emulsion. Here we are assuming that water flow is fully coupled to oil flow. An analogous assumption was made by Dehghanpour and DiCarlo (2013) who measured and modeled coupled flow of water and mobilized oil in a tertiary gas flood. We also assume that the size of water droplets is comparable to that of typical pore-throat in oil sand deposits.

Combining Eq.4 with Eq.6 gives

$$q_o = \int_0^{\infty} \frac{k\, S_o\, \rho_{em}\, g \sin\theta \left(\frac{\mu_w}{\mu_s}\, \delta^{-m} + 1\right)}{\mu_w + \mu_s \delta^m + (2.5\mu_w + \mu_s \delta^m)[(1 - S_{or}) - (S_{io} - S_{or})(1 - \delta^{-1})]} d\varepsilon \tag{11}$$

The emulsion density, ρ_{em}, as a function of distance beyond the steam chamber edge is given by

$$\rho_{em} = \rho_w S_w + \rho_o (1 - S_w) = (\rho_w - \rho_o) S_w + \rho_o \tag{12}$$

Combining Eq.12 with Eq.3 gives

$$\rho_{em} = (\rho_w - \rho_o) * \left[(1 - S_{io}) + (s_{io} - s_{or})\left(e^{-U\varepsilon/\alpha}\right)\right] + \rho_o \tag{13}$$

Substituting Eq.13 into Eq. 11 and re-arranging gives

$$q_o = \frac{k\, g \sin\theta}{\mu_S U} \beta \tag{14}$$

Where $\beta = \int_1^{\infty} \frac{S_o\left(\frac{a\mu_w}{\delta^{m+1}} + \frac{a\mu_s}{\delta} + \frac{\rho_o \mu_w}{\delta^m} + \rho_o \mu_s\right)}{\mu_w \delta + \mu_s \delta^{m+1} + 2.5(S_{io} - S_{or})\mu_w + \mu_s (S_{io} - S_{or})\delta^m} d\delta$ and $a = (\rho_w - \rho_o)(S_{io} - S_{or})$. This equation is not the final solution for oil flowrate since U and Sin θ are unknown.

4.1.3 Material balance

From the material balance, the rate of increase of oil flow across the differential element displayed in Figure 7, is related to the advance rate of the steam chamber interface. The material balance relationship can be expressed as

$$\frac{\partial q_o}{\partial x} = \emptyset\, \Delta S_o \left(\frac{\partial y}{\partial t}\right) \tag{15}$$

The advance velocity of interface, U, is given by

$$U = -\cos\theta \frac{\partial y}{\partial t} \tag{16}$$

U is growth velocity normal to the edge of steam chamber.

Substituting Eq. 15 and Eq. 16 into Eq. 14, and recalling that $\frac{\sin\theta}{\cos\theta} = \frac{\partial y}{\partial x}$, results in:

$$q_o \, \partial q_o = \frac{k\, g \sin\theta\, \beta\, \emptyset\, \Delta S_o}{\mu_s} \partial y \tag{17}$$

Integrating the left side of Eq. 17 from 0 to q_o and the right side from 0 to h (the height of steam chamber) gives the total oil flow rate per unit well length for one side of the steam chamber. Therefore, the total volumetric oil flow rate is given by

$$Q_o = 2L \sqrt{\frac{2\, k\, g \sin\theta\, \beta\, \emptyset\, \Delta S_o}{\mu_s}}$$

Here β accounts for in-situ emulsification phenomenon and replacing it with $\frac{\alpha}{m}$ gives Butler's original solution.

4.2 Model Results

4.2.1 Model Verification

Table 1 lists the parameters from a physical model experiment (Sasaki et al. 2001), which are used in the model verification and sensitivity analysis.

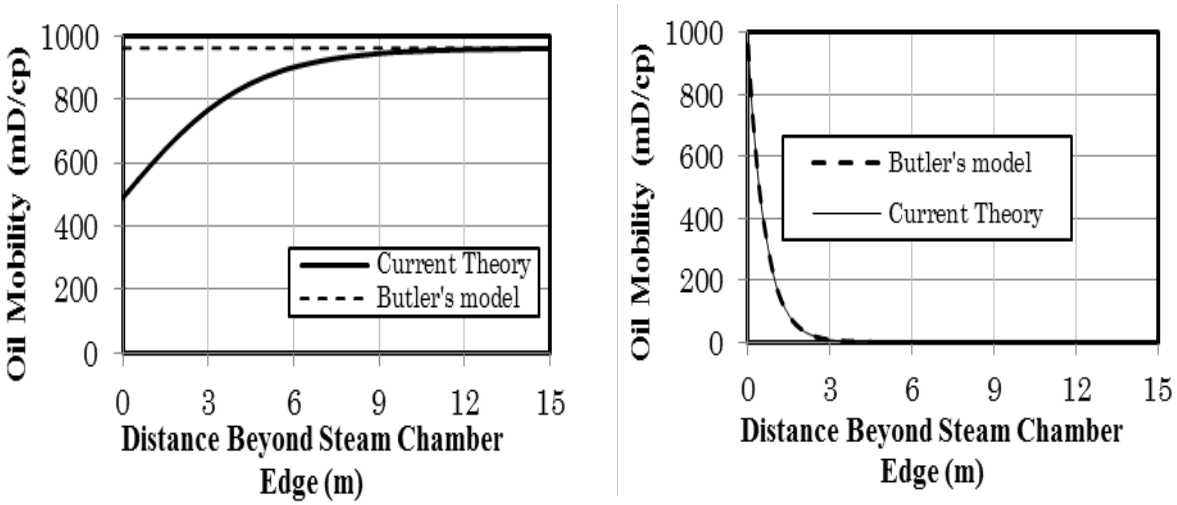

(a) (b)

Figure 8: Comparison of oil phase mobility from Butler's, and the current theory with respect to distance beyond the edge of a steam chamber using Sasaki et al. (2001) experimental data, (a) with no temperature effect, (b) with no emulsion effect.

Table 1: Parameters from Sasaki et al. (2001) Experimental Data

Parameters	Value
T_r (°C)	20
T_s (°C)	106
ρ_o (kg/m^3)	998
h (m)	0.3
L (m)	0.0045
∅	0.38
α (m^2/s)	2.60x10^{-7}
k_{ab} (m^2)	1.15x10^{-10}
K_{ro}	0.4
S_{io}	1
S_{orw}	0.05
S_{wc}	0
ν_s (m^2/s)	1.2010x10^{-4}
m	3.6
a	1

Figure 8 (a) compares the proposed model with Butler's model in the absence of temperature effect (*m*=0). The current model converges to Butler's model far enough from the chamber edge. As the distance increases, emulsion concentration approaches to zero, so there is no emulsion effect in the formation and the proposed model converges to Butler's single-phase model as expected. Figure 8 (b) compares the current model with Butler's, in the absence of emulsion effect. Emulsion viscosity is the same as oil viscosity and the emulsion mobility curve are exactly the same for the two models, so the current model matches with Butler's model.

Figure 9 compares the oil phase mobility with respect to distance beyond the interface estimated using 1) the proposed model, 2) Butler's model, and 3) Sharma and Gates' model. The results show that the oil mobility at any distance calculated from the proposed model is lower than that from Butler's model, and higher than that from Sharma and Gates' model. The oil phase mobility in the proposed model exponentially decreases with increasing distance, which is similar to Butler's but smaller due to the effect of emulsification. Because there is no consideration of multiphase and emulsion effect, Butler's model has the highest oil mobility. When there is no other fluid, the pore network is exclusively available for oil flow. Sharma and Gates considered multiphase effect by adding relative permeability to Butler's model. Multiphase assumption, allocates a share of fluid path to oil in Sharma and Gates' model. Therefore, the oil mobility in their model is lower than that in Butler's. Though emulsion increases effective oil viscosity, our model has a higher mobility than Sharma and Gates' model because we ignore multiphase effect in the presence of emulsion.

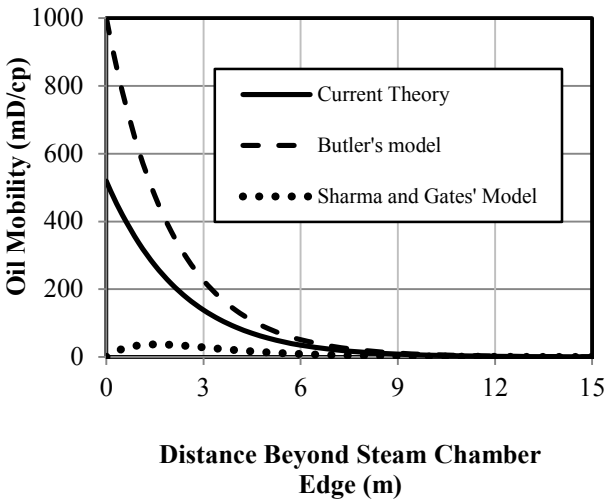

Figure 9: Comparison of emulsion mobility with respect to ε from Butler's, Sharma and Gates', and the proposed model using Sasaki et al. (2001) experimental data.

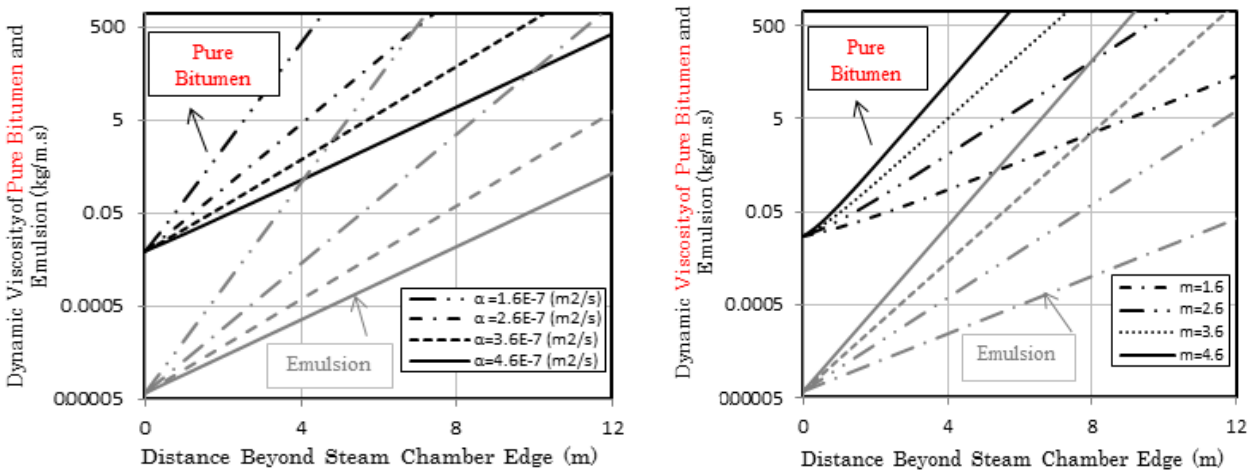

Figure 10: Dynamic Viscosity of pure bitumen and emulsion with respect of distance beyond edge of steam chamber for different values of (a) m and (b) α.

4.2.2 Sensitivity Analysis

In this part, we conduct a sensitivity analysis to investigate the dependence of oil flux and total oil production rate on m, α and μ_{water} which control emulsion viscosity.

4.3 Dynamic Emulsion Viscosity

Figure 10 shows how the viscosity of emulsion and pure bitumen change with respect to the distance from the chamber edge at different values of (a) α and (b) m. At a specific distance, μ_{em} increases by increasing m, while μ_{em} decreases by increasing α. Furthermore, μ_{em}- ε is steeper at lower values of α and at higher values of m.

4.4 Emulsion Mobility

Effect of m: Figure 11 (a) shows the effect of m on the oil mobility versus distance. The results reveal that the smaller the m, the larger the oil mobility is. As we described in previous section, increasing m increases μ_{em}, so the oil mobility

will be lower due to higher μ_{em}. Oil mobility increases with increasing temperature, as a result of decreasing viscosity.

Effect of α: Figure 11 (b) shows the oil mobility with respect to distance at several thermal diffusivities. Increasing α enhances the efficiency of heat transfer, and therefore, increases the oil mobility.

Effect of μ_w: Figure 11 (c) shows that μ_w does not have any significant effect on oil mobility. μ_w is significantly smaller than bitumen viscosity, and thus, it does not affect the oil mobility. Furthermore, based on Eq.5, the multiplier of oil viscosity is orders of magnitude larger than that of water viscosity ($e^{\left(\frac{U\varepsilon}{\alpha}\right)m} >> 1 >> e^{\left(-\frac{U\varepsilon}{\alpha}\right)m}$).

4.5 Volumetric Oil Flux

Figure 12 (a) to (d) compares the effects of α, U, m, and μ_w on volumetric oil flux, respectively. As expected, increasing α increases the oil flux due to faster heat transfer, and increasing m decreases the oil flux as oil becomes more viscous. Increasing U gives lower oil flux, since there will be less time to receive condensate thermal energy. As mentioned before, μ_w does not affect the oil mobility, and thus, changing water viscosity does not considerably affect volumetric oil flux.

4.6 Field data analysis

In this section, we use the proposed model to predict oil production rate at the field scale. Figure 13 compares the oil production rate by the proposed model with Butler's (1985) and Sharma and Gates' (2010) models, for six different field production data. Properties of the 6 fields are listed in Table 2. Butler's model overestimates the oil production rate, because there is no consideration of emulsion and multiphase effects. Oil flows easily because there is no relative permeability effect to limit the oil flow. Therefore, the values estimated by Butler's model are higher than those predicted by the other two models. Sharma and Gates considered multiphase effect in their model by adding relative permeability to Butler's model.

Their model has more accurate results than Butler's, but it does not consider emulsion effect which many authors reported in their observations.

The results reveal that the proposed model provides an improved estimate of oil production rate, under a series of specific values of α and m reported from field data of Athabasca deposit. It demonstrates that emulsification effect at the edge of steam chamber should be included in the SAGD analysis. Our model assumes that the entire flow system is single phase. Hence, there is a potential that this model overestimates the oil flow rate.

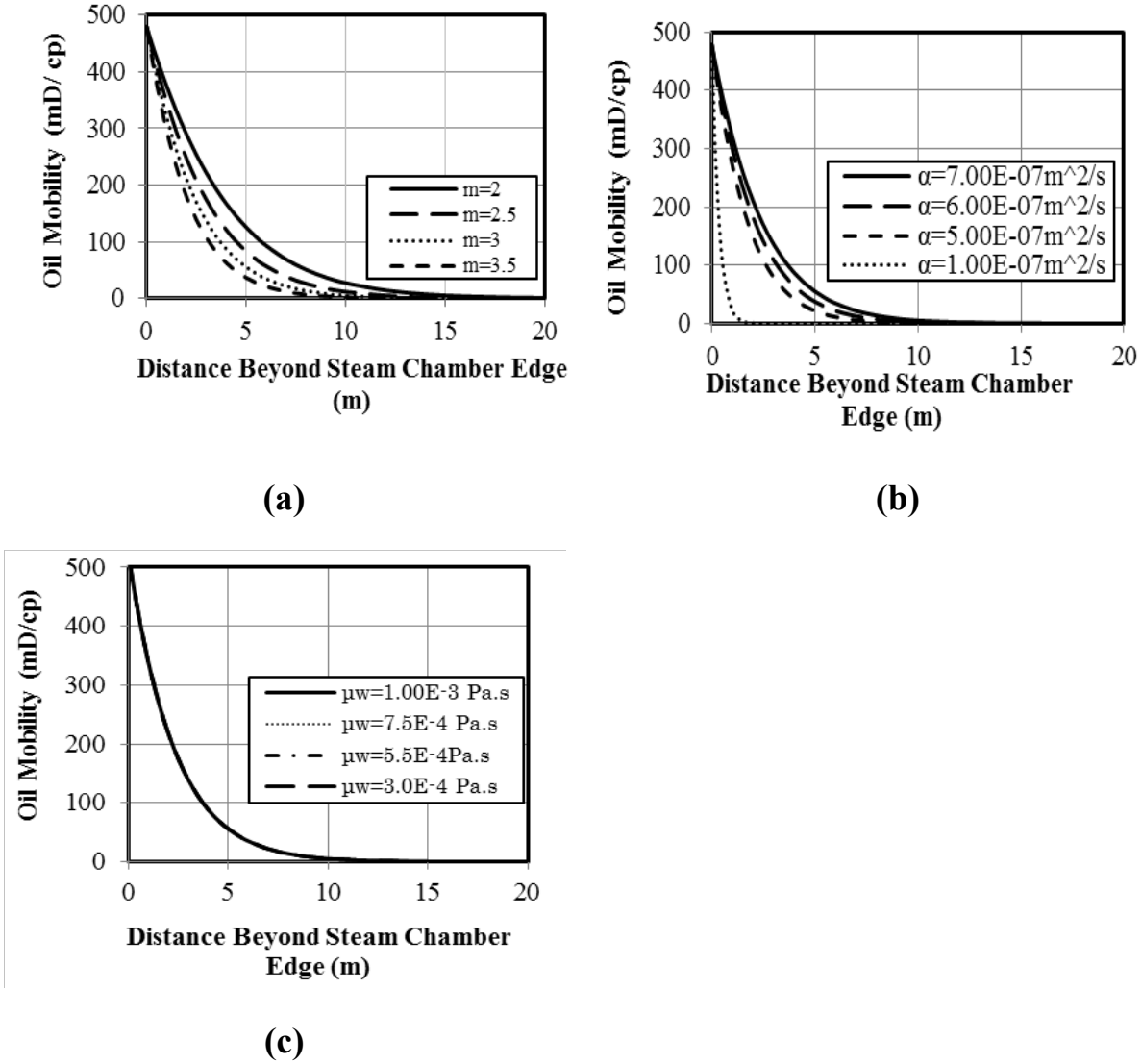

Figure 11: (a) Effect of temperature viscosity parameter (m), (b) thermal diffusivity (α), and (c) water viscosity (µw) on oil mobility with respect to distance beyond the edge of the steam chamber.

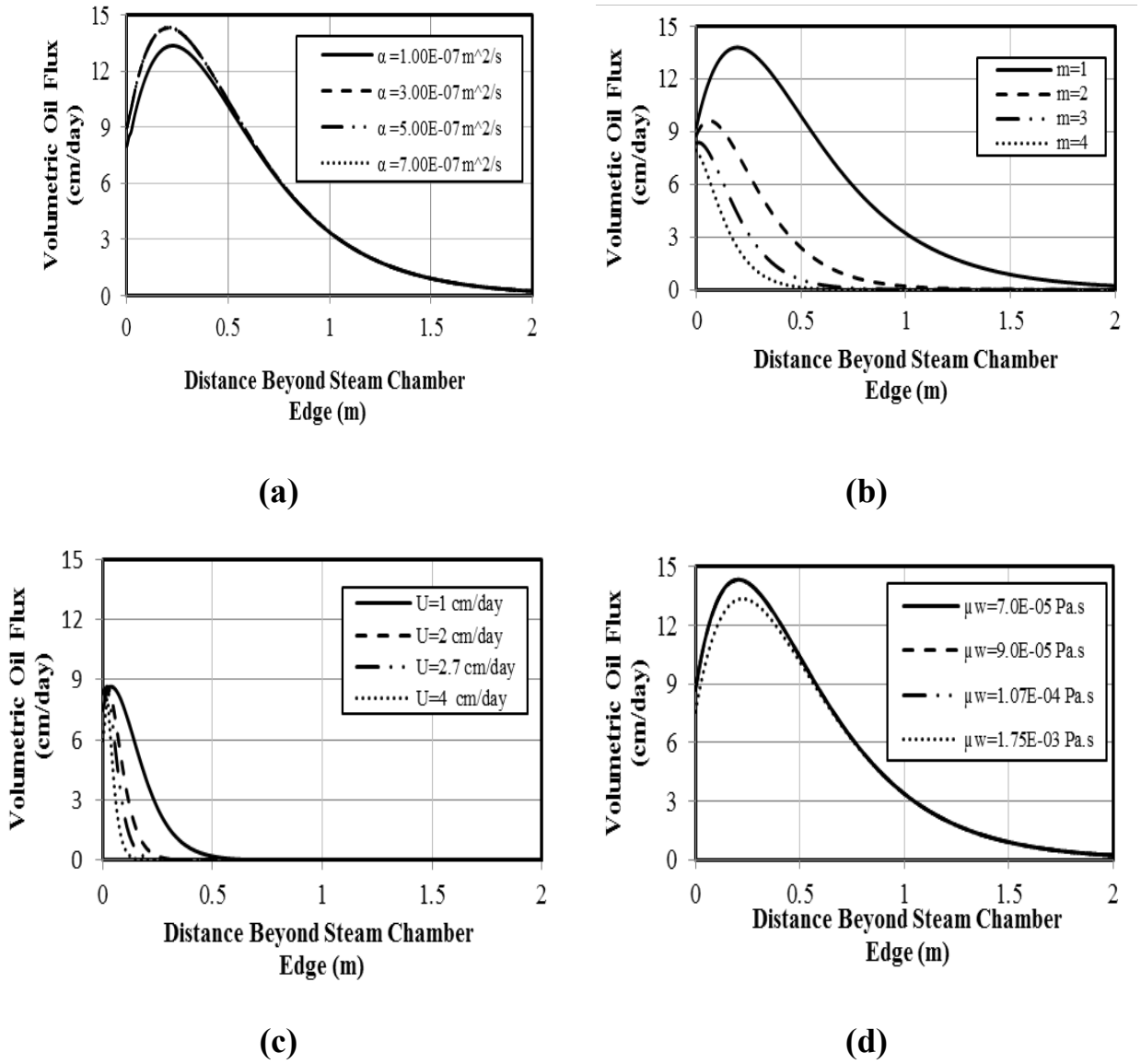

Figure 12: Effect of (a) thermal diffusivity (b) advance velocity of steam chamber (c) temperature viscosity parameter and (d) water viscosity on volumetric oil flux profile for Christina Lake reservoir.

(a) (b)

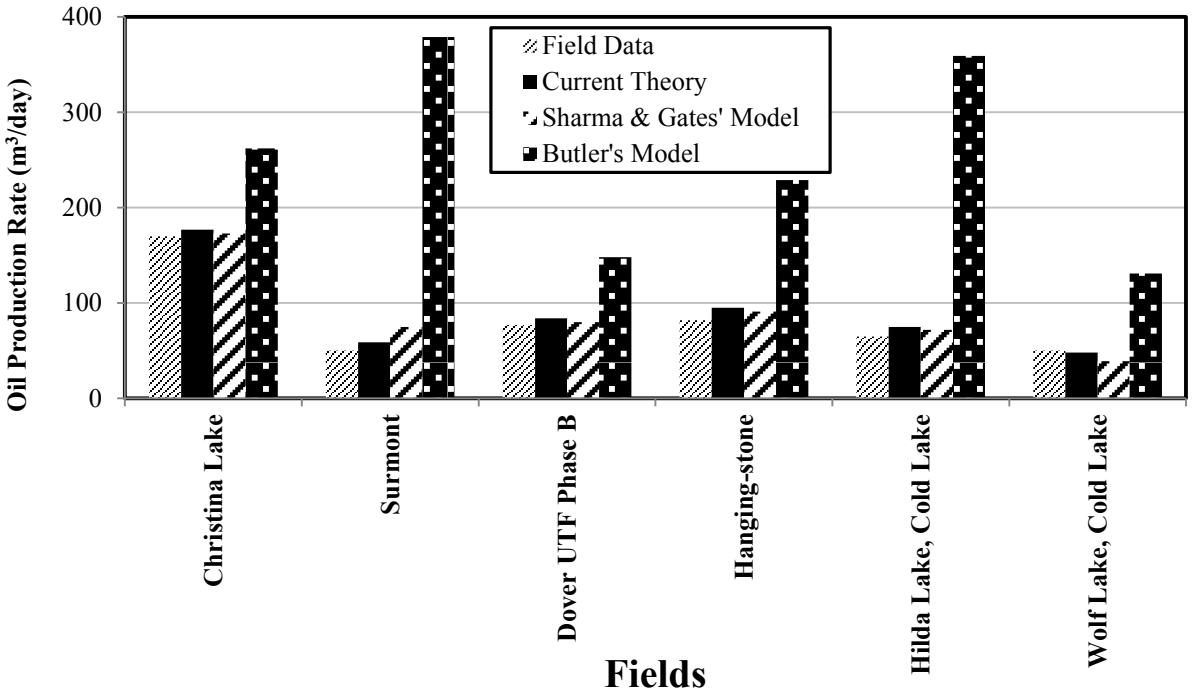

Figure 13: Comparison of SAGD models for different field operations data.

Table 2: Comparison of SAGD models for different field operations data (After Sharma and Gates 2010).

Wellpair	**A3**	**A**	**Phase B, Average of 3 well pairs**	**Average of 15 well pairs A, B, C, D, E,G, H, I,J, K, L,M, N, O, P & Q**	**I3/P3**	**B10 grand rapids, SD9 pad, average of 6 well pairs**
Parameters	**Christina Lake**	**Surmont**	**Dover UTF Phase B**	**Hangingstone**	**Hilda Lake, Cold Lake**	**Wolf Lake, Cold Lake**
T_R	20	15	7	20	20	20
T_s	220	225	220	260	245	250
ρ_s (kg/m^3)	880	880	880	980	880	980
ρ_o (kg/m^3)	1009	1009	1009	1015	1009	1015

h (m)	26	30	21	25	24	11
L (m)	690	850	500	500	1000	500
ϕ	0.33	0.33	0.33	0.35	0.35	0.32
α (m^2/s)	5.501×10^{-7}	0.201×10^{-7}	3.601×10^{-7}	2.60×10^{-7}	0.36×10^{-7}	3.00×10^{-7}
k_{ab} (m^2)	6.0×10^{-12}	5.0×10^{-12}	7.0×10^{-12}	5.0×10^{-12}	5.0×10^{-12}	3.0×10^{-12}
K_{ro}	0.2	0.2	0.2	0.3	0.2	0.3
S_{io}	0.80	0.79	0.85	0.77	0.63	0.75
S_{orw}	0.1	0.12	0.15	0.1	0.12	0.1
S_{wc}	0.15	0.1	0.1	0.1	0.1	0.1
ν_s (m^2/s)	6.81×10^{-6}	3.41×10^{-6}	7.95×10^{-6}	4.28×10^{-6}	3.41×10^{-6}	4.08×10^{-6}
m	4	5	5	5	5	4
μ_w (kg/m.s)	0.00085	0.00096	0.00117	0.00085	0.00085	0.00085
ρ_w (kg/m^3)	998	999	999	998	998	998
Oil flow rate q (m^3/day)						
Field data	**170**	**50**	**77**	**82**	**65**	**50**
Butler et al. (1981)	262	379	148	229	359	131
Sharma and Gates	173	75	80	91	72	39
Current Theory	**177**	**59**	**84**	**95**	**75**	**48**

5 Chapter 5: Two Phase Analytical Modeling of SAGD

The purpose of this chapter is to modify the single phase gravity drainage model developed in previous chapter to derive a two phase model. The model includes the effect of multi-phase flow (relative permeability) and oil saturation on oil mobility and drainage rate.

Assumptions of the model are as follow:

1. The reservoir is homogeneous.
2. Steam depletion chamber is symmetric and two dimensional.
3. Some part of the water is flowing separately and the rest is emulsified in oil.
4. Heat transfer ahead of the chamber edge is only by conduction.
5. Porous medium is homogeneous (constant porosity and permeability).
6. Heat losses are neglected.
7. Density is dependent on temperature.
8. Steam chamber that has reached the maximum height, *h*, and is expanding at a constant velocity *U*, in the direction perpendicular to the chamber walls.
9. Reservoir oil does not have any solution gas.
10. Heat transfer and mass transfer is directed normal to the edge of the chamber.

5.1 Proposed Theory

Figure 14 shows a conceptual model of a differential element at the edge of the steam chamber. In this model, portion of the water in the formation is assumed to be emulsified in the oil phase (C_w) and the rest is flowing along with as a continuous phase (S_w). The total water saturation (S_{wt}) becomes

$$S_{wt} = C_w + S_w$$

Probability of Emulsion formation decreases at higher temperatures, since when temperature increases emulsion concentration decreases. Water saturation is maximum at the chamber edge ($\varepsilon = 0$) and it equals to the connate water saturation far enough from the edge. Emulsion formation occurs more when there is less water saturation, water droplets can coalescence and flow as a continuous phase

when the water saturation is higher. As discussed in chapter 3 , emulsification phenomena is a function of following factors, temperature viscosity parameter, temperature, initial water saturation, steam injection rate, water droplet size and temperature diffusivity parameter.

Emulsion at the steam chamber interface is a system of immiscible fluids, with water droplets as the dispersed phase, and oil as the continuous phase. Therefore, if we assume, $\tau = \frac{\mu_{dispersed}}{\mu_{continuous}} = \frac{\mu_w}{\mu_o}$, and $x = C_w$, Taylor equation becomes

$$\frac{\mu_{em}}{\mu_o} = 1 + \left[2.5\left(\frac{\frac{\mu_w}{\mu_o} + 0.4}{\frac{\mu_w}{\mu_o} + 1}\right)\right] C_w \qquad (1)$$

There are several other equations for calculating emulsion viscosity at certain conditions.

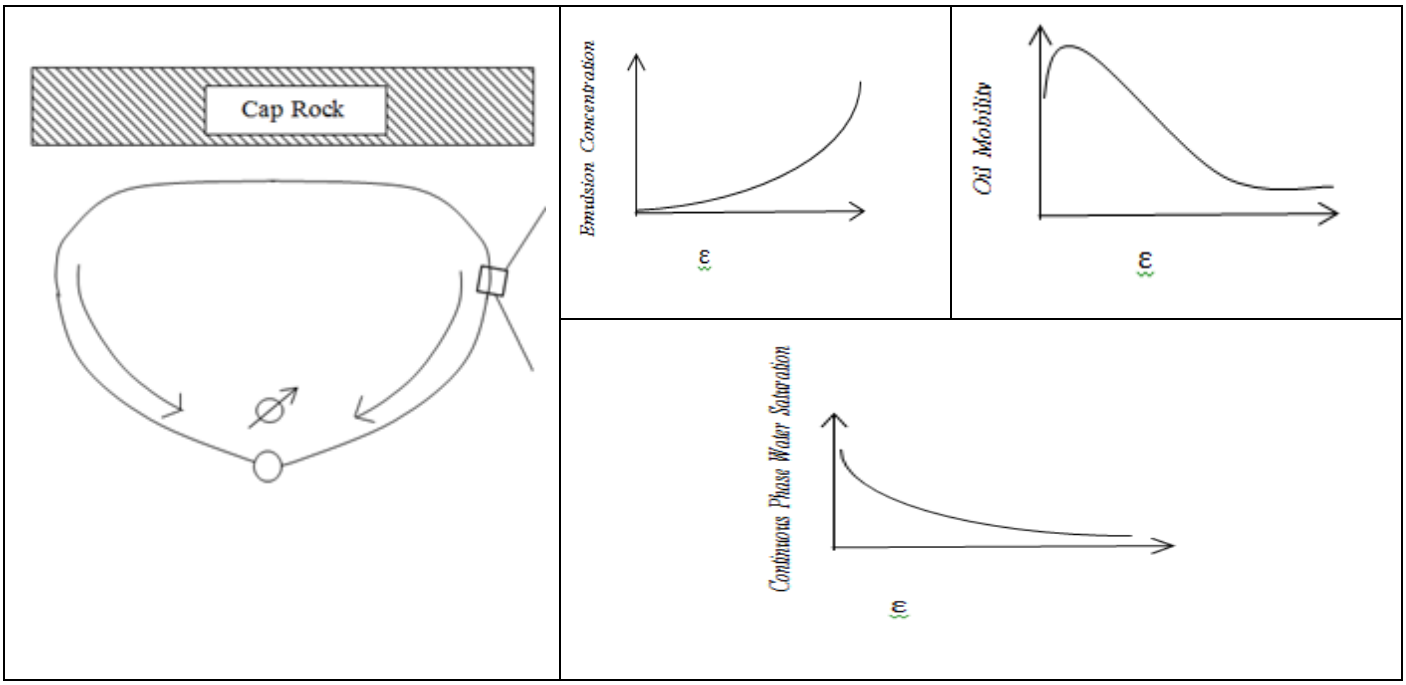

Figure 14: Schematic illustration of emulsion concentration, continuous phase water saturation, oil mobility and probability of emulsion formation function with respect to the distance beyond the steam chamber edge (ε).

Again, water saturation becomes a function of distance (ε) beyond the steam chamber interface.

$$S_w = 1 - S_o - C_w = (1 - S_{or}) - (S_{io} - S_{or})(1 - T^*) - C_w = (1 - S_{or}) - (S_{io} - S_{or})\left(1 - e^{\left(-\frac{U\varepsilon}{\alpha}\right)}\right) - C_w \quad (2)$$

Therefore, emulsion mobility defined by $\lambda_{oil} = \frac{k\,k_{row}}{\mu_{mix}} = \frac{k\,k_{row}}{\rho_{mix}\nu_{mix}}$ is given by

$$\lambda o = \frac{k\,k_{row}}{\mu_{mix}} = \frac{kk_{rocw}\left(\frac{S_{io}+C_w-S_{or}}{1-S_{wc}-S_{or}}\right)^a (1-(e^{-\frac{U\varepsilon}{\alpha}}))^a}{\mu_{mix}} = \frac{kk_{rocw}(1-(e^{-\frac{U\varepsilon}{\alpha}}))^a(\frac{\mu_w}{\mu_s}\left(e^{\frac{-U\varepsilon}{\alpha}}\right)^m + 1)}{\mu_w + \mu_s(e^{\frac{U\varepsilon}{\alpha}})^m\frac{\rho_o}{\rho_s} + C_w\left(2.5\mu_w + \mu_s\frac{\rho_o}{\rho_s}(e^{\frac{U\varepsilon}{\alpha}})^m\right)} \quad (3)$$

Where oil relative permeability and dimensionless water saturation are defined as Equation 4 and 5

$$k_{row} = k_{rocw}(1 - S_{wD})^a \quad (4)$$

$$S_{wD} = \frac{S_w - S_{wc}}{1 - S_{wc} - S_{or}} = \frac{S_{wt} - S_{wc} - C_w}{1 - S_{wc} - S_{or}} \quad (5)$$

5.1.1 Total oil flow rate

To develop an expression for the total oil flow rate we combine Darcy's and mass conservation laws together.

5.1.2 Darcy's law

Integration of differential Darcy's law equation for emulsion flow results in:

$$q_o = k_{rw}S_o\, g \sin\theta \int_0^{\infty} \frac{d\varepsilon}{\nu_{em}} = \quad (6)$$

$$q_o = kk_{rocw} g \sin\theta \int_0^{\infty} \frac{\left(\frac{S_{io} + C_w - S_{or}}{1 - S_{wc} - S_{or}}\right)^a (1 - (e^{-\frac{U\varepsilon}{\alpha}}))^a S_o \rho_{em}}{\mu_{em}} d\varepsilon$$

$$\rho_{em} = \rho_w S_w + \rho_o (1 - S_w) = (\rho_w - \rho_o) S_w + \rho_o \quad (8)$$

Combining equation 1 and equation 8 gives

$$\frac{\rho_{em}}{\mu_{em}} = \frac{[(\rho_w - \rho_o)((1 - S_{or}) + (S_{io} - S_{or})(1 - e^{-\frac{U\varepsilon}{\alpha}})) - C_w)] + \rho_o}{\frac{\mu_w + \mu_o + (2.5\mu_w + \mu_o) C_w}{\left(\frac{\mu_w}{\mu_o} + 1\right)}} \quad (9)$$

Substituting equation 9 in equation 8 gives

$$q_o = kk_{rocw} g \sin\theta \times \quad (10)$$
$$\int_0^{\infty} \frac{\left(\frac{S_{io} + C_w - S_{or}}{1 - S_{wc} - S_{or}}\right)^a (1 - (e^{-\frac{U\varepsilon}{\alpha}}))^a S_o ([(\rho_w - \rho_o)((1 - S_{or}) + (S_{io} - S_{or})(1 - e^{-\frac{U\varepsilon}{\alpha}})) - C_w)] + \rho_o) \left(\frac{\mu_w}{\mu_o} + 1\right)}{\mu_w + \mu_o + (2.5\mu_w + \mu_o) C_w} d\varepsilon$$

Let $\frac{U\varepsilon}{\alpha} = X$ then previous equation becomes below (Equation 11)

$$q = \frac{kk_{rocw}\, g \sin\theta \alpha}{U} \times \quad (11)$$
$$\int_0^{\infty} \frac{\left(\frac{S_{io} + C_w - S_{or}}{1 - S_{wc} - S_{or}}\right)^a (1 - (e^{-x}))^a S_o ([(\rho_w - \rho_o)((1 - S_{or}) + (S_{io} - S_{or})(1 - e^{-x})) - C_w)] + \rho_o) \left(\frac{\mu_w}{\mu_o} + 1\right)}{\mu_w + \mu_o + (2.5\mu_w + \mu_o) C_w} dX$$

Repeating the material balance same as previous chapter, the rate of increase of oil flow across the differential element, is related to the advance rate of the steam chamber interface.

$$\frac{\partial q_o}{\partial x} = \emptyset \Delta S_o \left(\frac{\partial y}{\partial t}\right) \quad (12)$$

The advance velocity interface is

$$U = -\cos\theta \left(\frac{\partial y}{\partial t}\right) \quad (13)$$

$$\frac{\sin\theta}{\cos\theta} = \frac{\partial y}{\partial x} \tag{14}$$

Simplifying equation 11 knowing $e^x = \delta$ gives

$$q_o = \frac{kk_{rocw}\, g sin\theta\alpha}{U} \times \tag{15}$$

$$\int_1^{\infty} \frac{(1 - (\delta^{-1}))^a S_o((\rho_w - \rho_o)[(1 - S_{or}) + (S_{io} - S_{or})(1 - \delta^{-1}) - C_w] + \rho_o)\left(\frac{\mu_w}{\mu_o} + 1\right)}{(\mu_w + \mu_o + (2.5\mu_w + \mu_o)C_w)\delta}\, d\delta$$

Substituting equation 12 and 13 in equation 11 with using the geometrical relation of equation 15 gives the total volumetric oil flow rate as

$$q_o = 2L \times \tag{16}$$

$$\sqrt{kk_{rocw}\, sin\theta g \emptyset\alpha \int_1^{\infty} \frac{S_O^2(1 - (\delta^{-1}))^a((\rho_w - \rho_o)[(1 - S_{or}) + (S_{io} - S_{or})(1 - \delta^{-1}) - C_w] + \rho_o)\left(\frac{\mu_w}{\mu_o} + 1\right)}{(\mu_w + \mu_o + (2.5\mu_w + \mu_o)C_w)\delta}\, d\delta}$$

5.2 Model Result

5.2.1 Model Verification

Figure 15 compares the oil phase mobility with respect to distance beyond the interface estimated using 1) the proposed model (two phase flow), 2) Butler's model, and 3) Sharma and Gates' model. Same as single phase model in previous chapter, the oil mobility at any distance calculated from the proposed model is lower than that from Butler's model, and lower than that from Sharma and Gates' model.

5.2.2 Sensitivity Analysis

Sensitivity analysis is done to investigate the dependence of oil flux and total oil production rate on m, α and μ_{water} which control emulsion viscosity.

5.2.3 Emulsion Mobility

Effect of m: Figure 16 (a) shows the effect of m on the oil mobility versus distance. The results reveal that the smaller the m, the smaller the oil mobility profile is. As we described in previous section, increasing m increases μ_{em}, so the oil mobility will be lower due to higher μ_{em}.

Effect of α: Figure 16 (b) shows the oil mobility with respect to distance at several thermal diffusivities. Increasing α enhances the efficiency of heat transfer, and therefore, in a specific distance higher the. α equals higher oil mobility. The maximum oil mobility occurs closer to the edge when α is smaller.

Effect of μ_w: Figure 16 (c) shows that μ_w does not have any significant effect on oil mobility.

5.2.4 Field data analysis

In this section, we use the proposed model to predict oil production rate at the field scale. Figure 17 compares the oil production rate by the proposed model with Butler's (1985) and Sharma and Gates' (2010) models, for six different field production data. Butler's model overestimates the oil production rate, because there is no consideration of emulsion and multiphase effects. Oil flows easily because there is no relative permeability effect to limit the oil flow.

The results reveal that the proposed model provides an improved estimate of oil production rate, under a series of specific values of α and m reported from field data of Athabasca deposit. It demonstrates that emulsification effect at the edge of steam chamber should be included in the SAGD analysis.

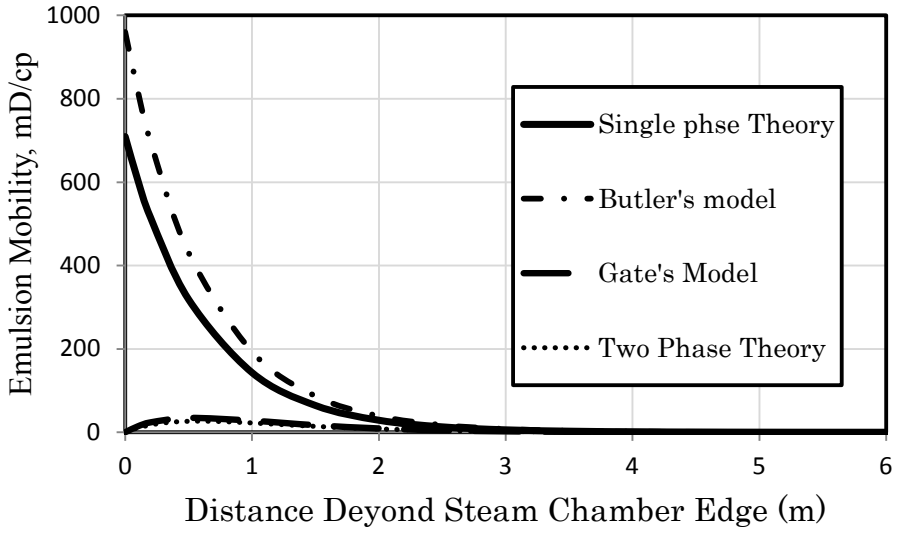

Figure 15: Comparison of oil mobility in different models.

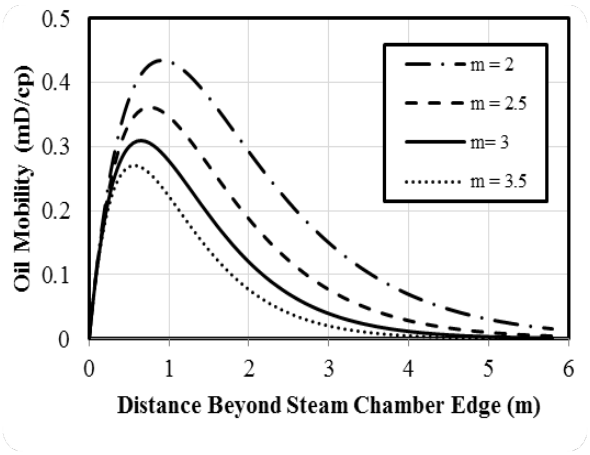

(a)

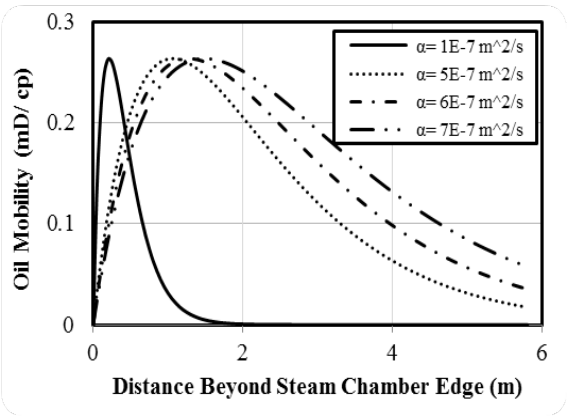

(b)

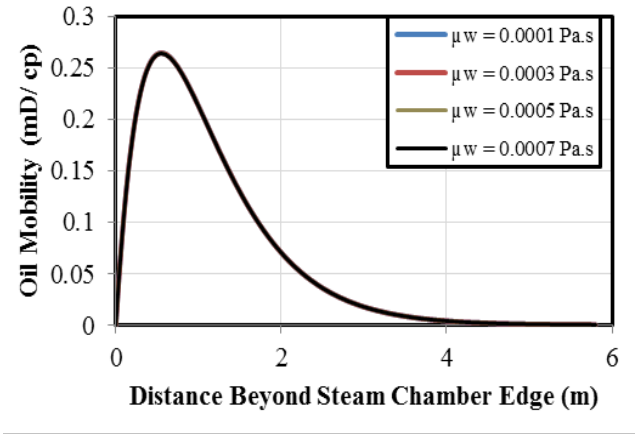

(c)

Figure 16: (a) Effect of temperature viscosity parameter (m), (b) thermal diffusivity (α), and (c) water viscosity (μw) on oil mobility with respect to distance beyond the edge of the steam chamber.

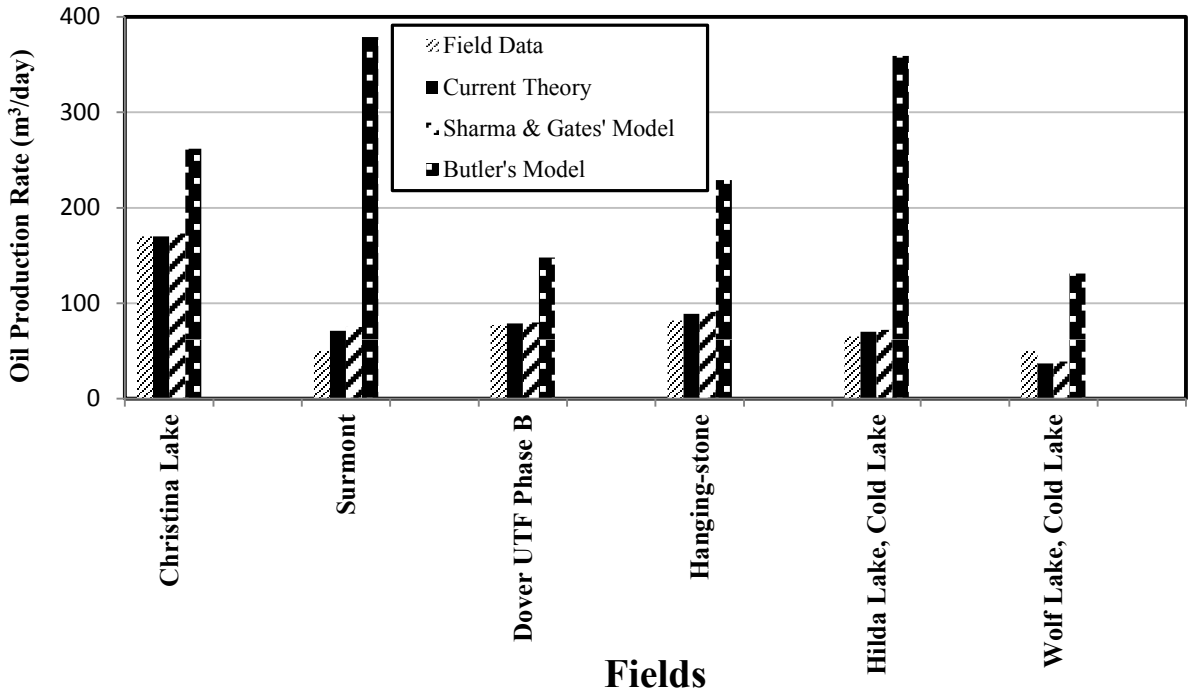

Figure 17: Comparison of SAGD models for different field operations data.

6 Chapter 6: Conclusion

An analytical model for lateral expansion of steam chamber during SAGD process is derived, with incorporation of formation and transport of water-in-oil emulsion. It is assumed that emulsion is generated due to condensation of steam penetrated into the heated bitumen. We also assume that the transport of emulsified water is fully coupled with that of the continuous oil phase, and therefore, use Darcy's law for modeling emulsion flow. The key mechanisms accounted for in this model are: alteration of bitumen viscosity and thermal effect. The new model reveals that the oil viscosity is set by the balance between temperature gradient due to heat conduction and microbubble concentration gradient due to emulsification. There are two controlling parameters, temperature-viscosity parameter and thermal diffusivity. A comparative application of the proposed model and other SAGD models on different field data reveals that emulsification effect should be included in the SAGD analysis. By considering emulsion in the proposed model, prediction of oil flow rate improved comparing with Butler's model. A need for extension of the model in case of extensive condensation and/or high initial water saturation made us to extend the single phase model. The extended model accounts for the flow of water as a separate continuous phase. It is assumed that emulsion is generated due to condensation of steam dispersed in oil phase while the rest of water condensation flows as a continuous phase. Considering emulsion in the proposed model improved oil flow rate prediction. The two phase model with emulsion effect simulates the real condition in the reservoir.

A more detailed analysis of effective parameters on emulsion formation in the reservoir during SAGD process is needed for further studies. Validation of the model with experimental data came from the laboratory would be valuable as well.

Nomenclature

a *Corey parameter (dimensionless)*
A_{m1} *Constant*
c_p *volumetric heat capacity of oil sands (J/m^3-deg Celsius)*
g *acceleration dure to gravity (m/s^2)*
h *reservoir thickness (m)*
H_f *heat trnsfered to residual oil, connate of warer and reservoir rock (J)*
H_o *heat transferred to the oil stream (J)*
H_r *heat tranasferred to oil saturated reservoir (J)*
k *permeability (m^2)*
k_{ab} *absolute permeability of the reservoir (m^2)*
k_{row} *relative permeability of oil with respect to water (dimensionless)*
k_{rocw} *relative permeability of oil at connate water saturation (dimensionless)*
k_{TH} *thermal conductivity (J/s m-deg Celsius)*
L *length of the production well (m)*
m *temperature viscosity parameter (dimensionless)*
Q *volumetric oil flow rate (m^3/s)*
q_o *oil flow rate per unit well length (m^2/s)*
$R_{g'}$ *weigthed (mass) steam oil ratio*
S_{io} *initial oil saturation (dimensionless)*
S_o *oil saturation (dimensionless)*
S_{or} *residual oil saturation (dimensionless)*
S_w *water saturation (dimensionless)*
S_{wc} *connate water saturation (dimensionless)*
S_{wD} *normalised water saturation (dimensionless)*
T *temperature (degree celsius)*
T^* *imensionless temperature (dimensionless)*
T_R *initial reservoir temperature (degree celsius)*
T_S *steam temperature (degree celsius)*
T_m *Temperature of heated bitumen (degree celsius)*
t *time (s)*
U *advanced velocity of steam chamber edge measured normal to the interface (m/s)*
V *rise velocity of steam chamber (m/s)*
x *distance measured in the horizontal direction (m)*
x_i *interface position (m)*
y *distance measured in the vertical direction (m)*
z *distance measured parallel to the well direction (m)*

Greek Symbols

α *thermal diffusivity (m^2/s)*
β *factor in flow rate equation with emulsion at the chamber edge*
Φ *porosity (dimensionless)*
μ_o *dynamic oil viscosity (kg/m.s)*
μ_s *dynamic steam viscosity (kg/m.s)*
μ_w *dynamic water viscosity (kg/m.s)*
μ_{em} *dynamic emulsion viscosity (kg/m.s)*

θ *angle between the steam chamber edge and the horizontal axis (dimensionless)*
ε *distance beyond the steam chamber edge measured in the direction normal to it (m)*
λ *latent heat of condensation (J/kg)*
λ_o *oil mobility (m^3s/kg)*
ν *dispersed phase volume fraction (dimensionless)*
υ_s *kinematic oil viscosity at steam temperature (m^2/s)*
υ_o *kinematic oil viscosity (m^2/s)*
ρ *rock density (kg/m^3)*
$\rho_c C_c$ *volumetric heat capacity of steam chamber excluding condensate ($kJ/°C\ m^3$)*
ρ_o *oil density (kg/m^3)*
$\rho_o C_o$ *volumetric heat capacity of oil*
ρ_{em} *emulsion density (kg/m^3)*
ρ_w *water density at reservoir temperature (kg/m^3)*
$\rho_w C_w$ *volumetric heat capacity of water*
ρ_s *bitumen density at steam temperature*

BIBLIOGRAPHY

1. Ahmed, M., Jaafar, M. Z., Wan Sulaiman, W. R., & Hashim, M. (2014, March). Miscible Flood Performance of Heterogeneous Layered Reservoirs: Considering Profile Control Through Controlled Fluid Movements. In Offshore Technology Conference-Asia. Offshore Technology Conference.

2. Alali, N., Pishvaie, M. R., & Jabbari, H. (2009). A new semi-analytical modeling of steam-assisted gravity drainage in heavy oil reservoirs. Journal of Petroleum Science and Engineering, 69(3), 261-270.

3. Akin, S. (2005). Mathematical modeling of steam assisted gravity drainage.SPE Reservoir Evaluation & Engineering, 8(05), 372-376.

4. Azad, A., & Chalaturnyk, R. J. (2010). A mathematical improvement to SAGD using geomechanical modelling. Journal of Canadian Petroleum Technology,49(10), 53-64.

5. Azad, A., & Chalaturnyk, R. J. (2012). An improved SAGD analytical simulator: Circular steam chamber geometry. Journal of Petroleum Science and Engineering, 82, 27-37.

6. Al-Bahlani, A. and Babadagli, T. (2009). SAGD laboratory experimental and numerical simulation studies: A review of current status and future issues. Journal of Petroleum Science and Engineering, 68(3-4), 135-150.

7. Azom, P. N., & Srinivasan, S. (2009, October). Mechanistic modeling of emulsion formation and heat transfer during the steam-assisted gravity drainage (SAGD) process. In SPE Annual Technical Conference and Exhibition. Society of Petroleum Engineers.

8. Azom, P. N. (2013). Improved modeling of the steam-assisted gravity drainage (SAGD) process, PhD thesis.

9. Azom, P. N., Kamp, A., & Srinivasan, S. (2013, June). Characterizing the Effect of Heat Transfer on Multiphase Flow during the Steam-Assisted Gravity Drainage (SAGD) Process. In SPE Heavy Oil Conference-Canada. Society of Petroleum Engineers.

10. Becker, J. R. (1977). Crude Oil Waxes, Emulsions, and Asphaltenes, Pennwell, Tulsa, OK, pp. 16–26, pp. 62–63, pp. 84–86.

11. Bharatha, S., Yee, C.-T., Chan, M.Y. (2005). Dissolved gas effects in SAGD, Paper 2005-176: Pet. Soc. 6th Canadian Int. Pet. Conf.
(56th Annual Tech. Meet.), Calgary Canada. June.
12. Birrell, G.E. (2001). 'Heat transfer ahead of a SAGD steam chamber: a study of thermocouple data from Phase B of the underground test facility (Dover Project)', SPE 71503: SPE Ann. Tech. Conf. And Exhib., New Orleans USA. Oct.

13. Bosch, R., Axcell, E., Little, V., Cleary, R., Wang, S., Gabel, R., & Moreland, B. (2004). A novel approach for resolving reverse emulsions in SAGD production systems. Canadian Journal of Chemical Engineering, 82(4), 836-839.

14. Brooks, R. H., & Corey, T. (1964). Hydraulic properties of porous media.

15. Broughton, G., & Squires, L. (1938). The viscosity of oil-water emulsions. Journal of Physical Chemistry, 42(1), 253-263.

16. Butler, R.M (1991). Thermal Recovery of Oil and Bitumen, Prentice-Hall, Englewood Cliffs, New Jersey.

17. Butler, R. M. (1985). New approach to the modelling of steam-assisted gravity drainage. Journal of Canadian Petroleum Technology, 24(3), 42-51.

18. Butler, R. M. (1987). Rise of Interfering Steam Chambers. Journal of Canadian Petroleum Technology, 26(3), 70-75.

19. Butler, R. M., McNab, G. S., and Lo, H. Y (1981). Theoretical studies of the gravity drainage of heavy oil during in-situ steam heating. Journal of Canadian Petroleum Technology, 59, 455-460.

20. Canbolat, S., Akin, S., & Kovscek, A. R. (2002). A study of steam-assisted gravity drainage performance in the presence of noncondensable gases. Paper presented at the Proceedings - SPE Symposium on Improved Oil Recovery, 78-89.

21. Cokar, M., Gates, I. D., & Kallos, M. S. (2013). A New Thermogeomechanical Theory for Gravity Drainage in Steam-Assisted Gravity Drainage. SPE Journal,18(04), 736-742.

22. Chung, K. H., & Butler, R. M. (1988). Geometrical effect of steam injection on the formation of emulsions in the steam-assisted gravity drainage process. Journal of Canadian Petroleum Technology, 27(1), 36-42.

23. Dehghanpour, H., DiCarlo, D. A. (2013). Drainage of capillary-trapped oil by an immiscible gas: Impact of transient and steady-state water displacement on three-phase oil permeability. Transport in Porous Media, 100, 297-319.

24. Ezeuko, C. C., Wang, J., & Gates, I. D. (2013). Investigation of Emulsion Flow in Steam-Assisted Gravity Drainage. SPE Journal, 18(03), 440-447.

25. Farah, M. A., Oliveira, R. C., Caldas, J. N., & Rajagopal, K. (2005). Viscosity of water-in-oil emulsions: Variation with temperature and water volume fraction. Journal of Petroleum Science and Engineering, 48(3-4), 169-184.

26. Farouq Ali, S.M. 2008. *Practical Heavy Oil Recovery*. ENCH 647 Lecture Notes, Dept. of Chem. and Pet. Eng., University of Calgary.

27. Heidari, M., Pooladi-Darvish, M., Azaiez, J., & Maini, B. (2009). Effect of drainage height and permeability on SAGD performance. Journal of Petroleum Science and Engineering, 68(1), 99-106.

28. Irani, M., & Cokar, M. (2014, June). Understanding the Impact of Temperature-Dependent Thermal Conductivity on the Steam-Assisted Gravity-Drainage (SAGD) Process. Part 1: Temperature Front Prediction. In SPE Heavy Oil Conference-Canada. Society of Petroleum Engineers.

29. Ito, Y., & Suzuki, S. (1999). Numerical simulation of the SAGD process in the Hangingstone oil sands reservoir. Journal of Canadian Petroleum Technology,38(09).

30. Kasenow, Michael. (2002).Determination of hydraulic conductivity from grain size analysis. Water Resources Publication.

31. Kokal, S. (2005). Crude-oil emulsions: A state-of-the-art review. SPE Production and Facilities, 20(1), 5-12.

32. Krieger, I. M., & Dougherty, T. J. (1959). A mechanism for non-Newtonian flow in suspensions of rigid spheres. Transactions of The Society of Rheology (1957-1977), 3(1), 137-152.

33. Noik, C., Dalmazzone, C., Goulay, C., & Glenat, P. (2005). Characterisation and emulsion behaviour of athabasca extra-heavy-oil produced by SAGD. Paper presented at the SPE/PS-CIM/CHOA International Thermal Operations and Heavy Oil Symposium Proceedings, , 2005 A365-A372.

34. Mehrotra, A. K., & Svrcek, W. Y. (1987). Viscosity of compressed cold lake bitumen. Canadian Journal of Chemical Engineering, 65(4), 672-675.

35. Mohammadzadeh, O., and Chatzis, I. (2009). Pore-level investigation of heavy oil recovery using steam assisted gravity drainage (SAGD). Paper presented at the Society of Petroleum Engineers - International Petroleum Technology Conference 2009, IPTC 2009, , 2 1070-1086

36. Mohammadzadeh, O., Rezaei, N., & Chatzis, I. (2010). Pore-level investigation of heavy oil and bitumen recovery using solvent -aided steam assisted gravity drainage (SA-SAGD) process. Energy and Fuels, 24(12), 6327-6345.

37. Murtaza, M., He, Z., & Dehghanpour, H. (2013). An approach to model three-phase flow coupling during steam chamber rise. Canadian Journal of Chemical Engineering.

38. Pal, R. (1998). A novel method to correlate emulsion viscosity data. Colloids and Surfaces A: Physicochemical and Engineering Aspects, 137(1), 275-286.

39. Poindexter, M. K., Chuai, S., Marble, R. A., & Marsh, S. (2006). The Key to Predicting Emulsion Stability: Solid Content. SPE Production & Operations,21(03), 357-364.

40. Rabiei Faradonbeh, M., Harding, T. G., & Abedi, J. (2014, June). Semi-Analytical Modeling of Steam-Solvent Gravity Drainage of Heavy Oil and Bitumen, Part 2: Unsteady-State Model with Curved Interface. In SPE Heavy Oil Conference-Canada. Society of Petroleum Engineers.

41. Ronningsen, H.P., (1995). Correlations for predicting viscosity of w/o emulsions based on North Sea crude oils. Proc. SPE Int.Symp., Oil Field Chem., SPE 28968, Houston, Texas

42. Sarbar, M. A., & Wingrove, M. D. (1997, January). Physical and chemical characterization of Saudi Arabian crude oil emulsions. In SPE Annual Technical Conference and Exhibition. Society of Petroleum Engineers.

43. Sasaki, K., Akibayashi, S., Yazawa, N., Doan, Q. T., & Farouq Ali, S. M. (2001). Experimental modeling of the SAGD process - enhancing SAGD performance with periodic stimulation of the horizontal producer. SPE Journal, 6(1), 89-97.

44. Sasaki, K., Akibayashi, S., Yazawa, N., Doan, Q., & Ali, S. F. (2001). Numerical and experimental modelling of the steam assisted gravity drainage (SAGD) process. Journal of Canadian Petroleum Technology, 40(1), 44-50.

45. Sasaki, K., Satoshi, A., Yazawa, N., & Kaneko, F. (2002, January). Microscopic visualization with high resolution optical-fiber scope at steam chamber interface on initial stage of SAGD process. In SPE/DOE Improved Oil Recovery Symposium. Society of Petroleum Engineers.

46. Sharma, J., & Gates, I. D. (2010). Multiphase flow at the edge of a steam chamber. Canadian Journal of Chemical Engineering, 88(3), 312-321.

47. Taylor, G. I. (1932). The viscosity of a fluid containing small drops of another fluid. Proceedings of the Royal Society of London. Series A, Containing Papers of a Mathematical and Physical Character, 41-48.

48. Wei, S., Lin-Song, C., Huang, S., & Huang, W. (2014, June). Steam Chamber Development and Production Performance Prediction of Steam Assisted Gravity Drainage. In SPE Heavy Oil Conference-Canada. Society of Petroleum Engineers.